Title

Nano-enhanced solid-state hydrogen storage: Balancing discovery and pragmatism for future energy solutions

Journal

Nano Research, 17(10)

ISSN
1998-0124

Authors

Dun, Chaochao
Wang, Xinyi
Chen, Linfeng
et al.

Publication Date
2024-10-01

DOI
10.1007/s12274-024-6876-y

Nano-Enhanced Solid-State Hydrogen Storage: Balancing Discovery and Pragmatism for Future Energy Solutions

Chaochao Dun [a,*], Xinyi Wang[b], Linfeng Chen[a], Sichi Li[c], Hanna M. Breunig[b], Jeffrey J. Urban[a,*]

[a] The Molecular Foundry, Lawrence Berkeley National Laboratory Berkeley, Berkeley, CA, 94720, USA

[b] Energy Analysis and Environmental Impacts Division, Lawrence Berkeley National Laboratory, Berkeley, CA, USA

[c] Lawrence Livermore National Laboratory, 7000 East Avenue, Livermore, CA 94550, USA

Corresponding authors: C. Dun (cdun@lbl.gov); J.J. Urban (jjurban@lbl.gov)

Abstract

Nanomaterials have revolutionized the battery industry by enhancing energy storage capacities and charging speeds, and their application in hydrogen (H_2) storage likewise holds strong potential, though with distinct challenges and mechanisms. H_2 is a crucial future zero-carbon energy vector given its high gravimetric energy density, which far exceeds that of liquid hydrocarbons. However, its low volumetric energy density in gaseous form currently requires storage under high pressure or at low temperature. This review critically examines the current and prospective landscapes of solid-state H_2 storage technologies, with a focus on pragmatic integration of advanced materials such as metal-organic frameworks (MOFs), magnesium-based hybrids, and novel sorbents into future energy networks. These materials, enhanced by nanotechnology, could significantly improve the efficiency and capacity of H_2 storage systems by optimizing H_2 adsorption at the nanoscale and improving the kinetics of H_2 uptake and release. We discuss various H_2 storage mechanisms—physisorption, chemisorption, and the Kubas interaction—analyzing their impact on the energy efficiency and scalability of storage solutions. The review also addresses the potential of "smart MOFs", single-atom catalyst-doped metal hydrides, MXenes and entropy-driven alloys to enhance the performance and broaden the application range of H_2 storage systems, stressing the need for innovative materials and system integration to satisfy future energy demands. High-throughput screening, combined with machine learning algorithms, is noted as a promising approach to identify patterns and predict the behavior of novel materials under various conditions, significantly reducing the time and cost associated with experimental trials. In closing, we discuss the increasing involvement of various companies in solid-state H_2 storage, particularly in prototype vehicles, from a techno-economic perspective. This forward-looking perspective underscores the necessity for ongoing material innovation and system optimization to meet the stringent energy demands and ambitious sustainability targets increasingly in demand.

Keywords: Nanomaterials, nanotechnology, solid-state H_2 storage, techno-economic analysis, model-driven material development processes

1. Introduction

The urgent global need to combat climate change has intensified the search for sustainable and efficient energy solutions, positioning H_2 as a pivotal carbon-free energy carrier in future energy systems.[1-3] As the lightest and most abundant element in the universe, H_2 offers a compelling energy solution, characterized by its high energy per mass—approximately 33.33 kWh/kg,[4] nearly three times higher than that of gasoline at about 12 kWh/kg,[5] and substantially higher than that of standard lithium-ion batteries at around 0.25 kWh/kg. This significant energy capacity positions H_2 not only as a versatile energy carrier but also as a crucial component for achieving carbon neutrality across various energy-intensive sectors such as transportation, industry, and electricity generation.[6] Moreover, H_2 storage solutions offer a strategic advantage in energy systems by providing the flexibility to manage varying power demands independently from the continuous energy flow that electrochemical devices typically require.[7] H_2 is unique in chemical energy storage modalities in that it can be cycled and used without significant degradation and maintains its capacity over long periods of inactivity. Such durability is crucial for applications such as grid-scale energy storage, or in cases where coupling to intermittent renewable energy sources is desired. Moreover, the capacity of H_2 for scaling is significantly superior to that of current battery technologies.[8] This difference illustrates the potential of H_2 to store much larger quantities of energy in a similar or smaller volume, making it particularly suited for large-scale storage needs.[9] Additionally, H_2 systems can possibly be designed to handle high peak power outputs without the risk of degrading the system's overall energy storage capacity. In contrast, lithium-ion batteries often face challenges with heat management and longevity when subjected to high discharge rates.[10] Therefore, H_2 storage not only provides high-capacity energy solutions but also offers system stability and durability benefits that are unique and complement other forms of energy storage such as batteries or pumped hydroelectric power. This combination of high energy density, scalability, and stability positions H_2 as a pivotal technology in the transition to renewable energy systems.

According to analyses by the U.S. Department of Energy (DOE), in order to make cost of H_2 storage cost-competitive (e.g. with batteries) for large-scale energy solutions, a proximate target \$/W cost is approximately \$162/kWh for a 100 MW system.[11] Achieving this cost reduction would significantly enhance the feasibility of H_2 as a key component of sustainable energy infrastructure. In this scenario, H_2 could provide a more durable and robust solution for systems requiring high power outputs intermittently, such as in backup power systems or renewable energy buffering.

H_2 is a versatile energy vector that can serve various roles in a future energy landscape. For example, H_2 could revolutionize energy systems by providing a viable alternative to fossil fuels in hard-to-decarbonize industries such as steel manufacturing, heavy transportation, and chemical production. Despite its potential, the deployment of H_2 technologies faces several challenges that must be addressed to fully harness its capabilities. There are significant challenges in the efficient production, transport, and storage of H_2. Here we focus on the latter of these problems – storage. The primary challenge is the low volumetric energy density of H_2 in its natural gaseous state, about 3 kWh/m^3, which necessitates storage under high pressure or liquefaction for practical uses. For example, the U.S. DOE has set targets for fuel cell vehicles onboard H_2 storage, requiring an initial system (including tank and materials) delivery capacity of 30 g/L (4.5 wt%) and an ultimate target of 50 g/L (6.5 wt%).[12] Therefore, in automotive applications, H_2 is often compressed to high pressures to enhance its volumetric energy density. At a pressure of 700 bar, typical for H_2 fuel cell vehicles, the volumetric energy density of H_2 can reach about 39.4 kWh/m^3, improving its suitability for storage and transport. Bulk storage is only commercial at pressures closer to 170 bar. In high-pressure gas storage, the method relies on robust high-pressure containers constructed from steel or advanced composite materials rather than requiring specific materials.[13] This type of H_2 storage necessitates sturdy and heavy tanks that can safely contain the gas at high pressures, significantly increasing the weight and cost of the storage systems. Additionally, maintaining such high pressures requires energy-intensive compression processes, which reduce overall energy efficiency and pose safety risks due to the volatile nature of compressed H_2.[14] Similarly, liquid H_2 storage employs specially engineered cryogenic containers, typically made from stainless steel or other alloys known for their exceptional performance at extremely low temperatures. This method faces significant challenges as well due to the low boiling point of H_2 (-252.9°C), necessitating sophisticated and energy-intensive cryogenic technology to maintain this temperature.[15] Furthermore, the insulation systems needed to minimize heat transfer and prevent H_2 evaporation add complexity and cost to the storage and transport infrastructure.[15] These challenges naturally lead to the exploration of solid-state H_2 storage solutions, which aim to provide safer and more efficient means to store H_2 without the need for high-pressure tanks or cryogenic temperatures.

Moreover, H_2 is increasingly recognized for its multifaceted role beyond transportation, especially in grid-scale energy storage and as a buffer for intermittent renewable energy sources like wind and solar. These renewable sources often produce energy that does not align with demand, making H_2 essential for stabilizing the energy grid. It can store excess energy during peak production and release it when demand exceeds the output from renewables. This capability not only helps manage fluctuations in energy supply but also ensures a constant and reliable energy flow for consumer and industrial needs.[16] Additionally, integrating H_2 into broader energy systems aids the decarbonization of sectors beyond transportation, including industrial processes and heavy machinery, which traditionally rely on fossil fuels. The versatility of H_2 thus extends its utility across various applications, positioning it as a cornerstone in the transition towards a more sustainable and resilient energy infrastructure. This expanding role highlights the critical need to develop advanced H_2 storage technologies to fully harness its potential as a green energy solution. A simple summary of advantages/limitations of traditional H_2 storage methods (e.g., high-pressure H_2 storage, liquid H_2 storage) and potential of solid-state H_2 storage technologies is given in **Table 1**. Here, we focus exclusively on solid-state H_2 storage, so liquid carriers such as ammonia, methanol, methylcyclohexane (MCH), and formate are not covered.

Table 1. Advantages/limitations of traditional H_2 storage methods (e.g., high-pressure H_2 storage, liquid H_2 storage) and potential of solid-state H_2 storage technologies.

Feature	High-Pressure H_2 Storage	Liquid H_2 Storage	Solid-State H_2 Storage
Safety Level	High (Requires containment at about 350-700 bar)	Medium (Requires storage at -253°C)	High (Stored in chemical bonds, reducing leakage risks)
Energy Density (MJ/kg)	5-10	~10	5-18 (Depends on the material, e.g., MOFs, metal hydrides)
H_2 Release Rate	Fast	Fast	Medium-Slow
Repeatability	High (>5000 cycles)	High (with evaporation losses)	Medium-High (Depends on the cycle stability of the material, e.g., MgH_2 shows good performance)
Cost	Medium (Requires high-pressure tanks and compressors)	High (Requires cryogenic cooling equipment)	High (Initial R&D costs for new materials, but potentially lower operational costs)

Solid-state H_2 energy storage, particularly using low-cost materials such as sorbents or metal hydrides that consist of earth-abundant elements, presents a significant advancement over traditional compressed H_2 gas storage methods. These alternatives offer superior volumetric energy density and require lower operational pressures. This shift promises enhanced safety and may lead to notable energy and cost efficiencies. Specifically, sorbent materials like zeolites and activated carbons capitalize on their large surface areas to adsorb H_2 at relatively low pressures and higher densities than compressed gas. For instance, advanced porous materials can adsorb H_2 up to 5-10 wt% under moderate pressure (around 20-50 bar), which is substantially less than the 350-700 bar pressures used in compressed H_2 storage.[17] Metal hydrides, for example, allow H_2 to be stored at densities comparable to liquid H_2 without the need for extreme pressures or low temperatures. For instance, magnesium hydride (MgH_2) offers a theoretical H_2 storage capacity of about 7.6 wt% and can store 110 kg/m^3.[18] This compares favorably to compressed H_2, which at 700 bar achieves about 40 kg/m^3. Moreover, metal hydrides can release H_2 at relatively moderate temperatures (200-300°C), which may be efficiently achieved using waste heat from industrial processes, further reducing operational costs.

The transition to advanced solid-state H_2 storage methods is crucial, as it aligns with global sustainability goals by enabling more efficient storage and transport of H_2. This enhances the broader adoption of H_2 as a key component of future clean energy systems. Importantly, these technologies are not merely theoretical but are actively being explored and deployed at a national scale. For instance, in 2023, Japan and South Korea committed to co-developing a H_2 and ammonia supply chain aimed at decarbonizing their energy bases. This initiative, known as the *Hydrogen Ammonia Global Value Chain*, marks a significant step toward sustainable energy practices. Moreover, the *Energy Earthshots Initiative*, launched by the U.S. DOE, is a comprehensive effort to drastically reduce the costs of clean energy technologies, making them more accessible and scalable across various sectors. One of its first targets, the "*Hydrogen Shot*," aims to lower the cost of clean H_2 to $1/kg within a decade—a substantial decrease from the current prices, which average around $5/kg for green H_2. The initiative focuses on fostering breakthroughs in H_2 production, storage, transport, and utilization technologies. By prioritizing cost reductions through innovations and economies of scale, it seeks to make H_2 a competitive option in the broader energy market.

With increasingly large-scale commitments to carbon-free H_2 energy, it is imperative to advance R&D goals further, as traditional solutions to H_2 storage often fall short without significant subsidies or carbon taxes.[19] In this context, nanomaterials offer a promising pathway to enhance the efficiency and capacity of storage systems by increasing the available surface area for H_2 adsorption. This enhancement is particularly crucial for metal hydrides or MOFs, where H_2 is either absorbed within the material or adsorbed on its surface. Nanomaterials can be engineered to optimize these interactions, potentially yielding more compact and efficient H_2 storage solutions. Additionally, nanotechnology can enhance the kinetics of H_2 uptake and release, accelerating the process to meet operational demands more effectively. The distinctive properties of nanomaterials, such as their high surface-to-volume ratios and customizable surface chemistries, make them exceptionally suited for improving these processes.

Over the past 5 to 10 years, material research often relied on freely allocated funding, lacking clear direction and efficiency considerations. Now, by incorporating techno-economic analysis (TEA) and model-driven material development processes, researchers can predict the performance and cost-effectiveness of materials more scientifically, thus driving R&D efforts more purposefully. Notably, comprehensive TEA remains a crucial tool for evaluating the methods and practical feasibility of solid-state H_2 storage, ensuring that both scientific and economic aspects are addressed to optimize the development process. One example of blending pragmatism with discovery, have been the multi-disciplinary research efforts occurring within the Hydrogen Materials Advanced Research Consortium (HyMARC). This is a DOE funded center which has explicitly prioritized the use of TEA, data- and sample-sharing, and partnership with private companies as part of a materials development and discovery effort. A key area of HyMARC's impact has been the development of advanced nanomaterials, including metal hydrides, complex chemical hydrides, and novel sorbents, which have been fundamental in addressing the volumetric and gravimetric efficiency, reversibility, and rates of H_2 adsorption and desorption challenges associated with H_2 storage.

This work aims to provide a comprehensive overview of the current state of H_2 as an energy carrier by interweaving threads of scientific innovation in nanomaterials and nanotechnologies with emerging information about real-world market requirements. We seek to offer researchers across the energy sector with a balanced and insightful perspective that combines elements of a traditional review approach with unique insights from our own research. It will unfold in three main sections: the first will discuss the fundamentals of solid-state H_2 storage in nanomaterials, covering weak to strong bonding and the primary challenges faced. The second section will meticulously analyze recent progress in nanotechnologies on a case-by-case basis, correlating the breakthroughs with some of the technical challenges discussed earlier. The final section will explore TEA with ongoing challenges and practical considerations, setting the stage for a discussion that not only reflects the current landscape but also outlines a forward-looking perspective on the pivotal role of nanomaterials and nanotechnologies in enabling H_2 as a sustainable energy carrier for the future.

2. Fundamentals of Solid-State H_2 Storage

The primary mechanisms of H_2 adsorption—Physisorption, Chemisorption, and Kubas Interaction—play distinct roles in H_2 storage technologies, offering varying bond strengths, reversibility, and energy requirements. These mechanisms underpin materials-based H_2 storage technologies, each with its intrinsic advantages and limitations, and each uniquely linked with the practical constraints of engineering and the performance of associated balance of plant processes such as refrigeration, compression, and heating. The enthalpy of adsorption (ΔH^o) serves as a key metric for characterizing H_2 storage materials, with an optimal range typically falling between 15 and 25 kJ mol^{-1} H_2 to maximize the deliverable capacity of the sorbent at ambient temperature. [20] Different mechanisms of H_2 adsorption correspond to distinct ranges of ΔH^o, as depicted in **Figure 1**, thereby introducing the initial set of pros and cons for each material class, which we will elaborate below.

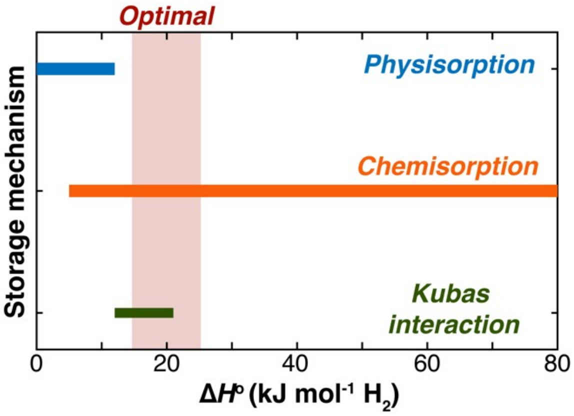

Figure 1. Primary mechanisms of H_2 adsorption: Physisorption, Chemisorption, and Kubas interaction, and their relationship with the enthalpy of adsorption (ΔH°).

Physisorption. Physisorption involves the physical adhesion of H_2 molecules to the surface of a material through weak intermolecular forces, such as van der Waals interactions, which include induced and instantaneous dipole-dipole attractions. Unlike chemisorption, physisorption does not involve the formation or breaking of chemical bonds, resulting in fast adsorption/desorption kinetics. However, the weak binding strengths associated with physisorption, exacerbated by the nonpolar nature of H_2, present inherent limitations to storage density. The low ΔH°, typically < 12 kJ mol^{-1} H_2 as **Figure 1** shows, characterizing physisorption diminishes further with increasing surface coverage, necessitating low temperatures or high pressures to achieve practical storage densities. Moreover, the strength of interactions varies heterogeneously across sorbent architectures, with only a fraction of locations exhibiting affinity for H_2. For instance, in MOFs, which have been extensively studied for H_2 physisorption, regions proximal to metal centers display notable H_2 attraction, while interactions rapidly diminish away from these sites. Consequently, the amount of stored H_2 initially increases sharply with pressure but decelerates as high-potential binding sites become saturated, compromising the usable capacity for each adsorption/desorption cycle. Identifying or designing new physisorbents with improved usable capacity typically involves several major strategies: (1) enhancing the chemistry of undercoordinated open metal sites (UOMs) to increase their affinity to H_2, (2) maximizing the crystallographic density of UOMs, and (3) developing smart nanomaterials with properties in response to specific environmental stimuli. These technical objectives have spurred the development of a workflow comprising high-throughput computational screening of MOF material space, target synthesis, and reliable adsorption experiments. In addition to conventional MOFs, there have been advancements in the development of novel flexible MOFs to address the issue of low usable capacity. Despite progress made, there are remaining challenges in both computational and experimental approaches. We will discuss these aspects further in **Section 3**.

Chemisorption. Chemisorption involves the formation of chemical bonds between H_2 and the absorbent material. Metal hydrides, borohydrides, amides, and their composites are significant components of solid-state H_2 storage materials in the realm of chemisorption. We will not focus on other terms such as "interstitial", where H_2 atoms occupy interstitial sites—spaces between metal atoms—in the crystal lattice of certain metals, in our discussion. Despite the typically strong chemical bonds formed between H_2 and metals in metal hydrides, ΔH° spans a wide range. **Figure 1** shows the ΔH° range for metal hydrides which we will focus on in this work. Identifying a metal hydride that exhibits both a favorable ΔH° and high gravimetric/volumetric H_2 storage capacity is desirable but challenging. In bulk form, most metal hydrides with high H_2 storage capacity have ΔH° values outside of the optimal range, either too low (e.g., AlH_3) or too high (e.g., $LiAlH_4$). Even if the capacity constraint is slightly eased, another significant hurdle lies in the sluggish kinetics of the H_2 uptake and release processes, which necessitate energydemanding high temperatures for practical operations. In this work, metal hydrides are further categorized into two subclasses: complex metal hydrides and light metal hydrides. For example, the formation of complex metal hydrides involves an extensive phase transformation where metal atoms bond with H_2, rearrange, and form a structure distinctly different from the original metal crystals. This transformation is responsible for the sluggish kinetics observed, and a deep atomistic understanding is significantly lacking. Additionally, many metals or alloys, such as Mg and TiFe,[21] tend to form passivation layers of metal oxides, which can be amorphous and exhibit heterogeneous compositions. These oxide layers often act as barriers, with the kinetics of H_2 dissociation and penetration through these layers being rate-determining before the H_2 reaches the bulk metal regions for storage. In some cases, however, controlled formation of these oxides can even facilitate surface H_2 association. Achieving a fundamental understanding of these complex chemical processes is technically challenging but crucial for making significant progress in chemisorption based H_2 storage technologies.

To enhance the performance of these materials, several major strategic approaches can be particularly effective. First, doping with catalysts such as transition metals can significantly enhance H_2 uptake and release kinetics by altering the electronic properties of the host material. This facilitates faster, more efficient H_2 absorption and desorption at lower temperatures. Second, reducing the material to nanoscale dimensions increases the surface area to volume ratio, providing more active sites for H_2 interactions. This can speed up the kinetics and may also improve the thermodynamics of the H_2 storage process, potentially lowering operational temperatures and enhancing energy efficiency. Implementing these strategies can accelerate advancements in chemisorption based H_2 storage, addressing key barriers to its widespread application.

Kubas interaction. The Kubas interaction is a special form of adsorption mechanism. In Kubas interaction, H_2 molecules are adsorbed through coordination with transition metal centers, but the H-H bonds of the H_2 molecules are not broken. This type of adsorption primarily involves the transfer of electron density from the σ bond of the H_2 molecule to the empty *d* orbitals of the metal (σ-bonding), and the back-donation of electron density from the metal to the antibonding σ^* orbital of the H_2 (back-donation). This interaction extends and weakens the H-H bond without completely breaking it. The advantage of Kubas interaction for H_2 adsorption is significant: it is stronger than physisorption and has the potential to reach the optimal range of ΔH^o without the need to undergo complex phase transformations. In theory, this mechanism allows for the reversible adsorption and release of H_2 under mild conditions without significant energy barriers, which is highly beneficial for practical H_2 storage applications. It enables effective storage and release of H_2 without requiring high temperatures or pressures. In practice, materials leveraging Kubas interactions still need to meet H_2 capacity requirements. A material with an unstable or low density of accessible Kubas sites would not be sufficient for real-world applications.

Nonetheless, there have been reports of new materials, such as MOFs and MXenes, with undercoordinated UOMs reactive enough to induce Kubas interactions with H_2 and exhibit favorable ΔH^o. While these early findings are exciting, further rigorous validation is necessary to confirm their potential for practical H_2 storage applications.

3. Progress in Solid-State H_2 Storage

Recent advances in materials science have significantly influenced the development of novel sorbents like MOFs and covalent-organic frameworks (COFs), metal hydrides, and complex chemical hydrides, pivotal in enhancing H_2 storage technologies. These materials have led to improvements in storage densities and kinetics, crucial for various small to medium sized (<100 tonnes of H_2 storage) practical applications ranging from mobile applications in fuel-cell-powered vehicles to stationary storage for grid management. Such enhancements are directly linked to the ability of these materials to utilize distinct H_2 adsorption mechanisms effectively.

Building on the understanding of different H_2 adsorption mechanisms and technical limitations briefly outlined in the previous section, we will now delve into a detailed, case-by-case analysis of the current progress in solid-state H_2 storage. We will explore how each primary mechanism—Physisorption, Chemisorption, and Kubas interaction—contributes uniquely to advancements in this field. By examining specific instances where these mechanisms have been effectively utilized, we can gain insights into their practical applications and potential for future innovations in H_2 storage technology in **Section 4**.

3.1 Physisorption

Physisorption has been the most extensively studied mechanism due to its operation at relatively low temperatures and pressures compared to chemisorption and compressed gas methods. In which, H_2 could be reversible storage and released by simply reducing the pressure or increasing the temperature, a feature crucial for practical applications.[22, 23] The binding energy is a key factor in distinguishing physical adsorption from chemisorption; in physisorption, each adsorbed entity typically has a binding energy ranging from 0.1 to 0.4 eV[24], which is significantly lower than the binding energy in chemisorption (>0.8 eV). Microporous materials with a high surface area, such as carbonaceous materials (graphene[25-29], carbon nanotube[30-33], and fullerenes[34]), MOFs[3, 35-39], COFs[40-43], zeolites[44, 45], and boron nitride (BN)[46-48] could physically adsorb a substantial quantity of H_2. Immaterial and Baker Hughes have made significant strides in physisorption-based solid-state H_2storage. Immaterial specializes in advanced porous materials like MOFs and COFs, optimized for efficient H_2 adsorption. Baker Hughes leverages their materials expertise to develop novel adsorbents tailored for high-pressure H_2 storage. Both companies demonstrate the practicality of physisorption for high-density H_2 storage, advancing its commercial potential in diverse industries.

Nevertheless, the major concerns in physisorption for solid-state H_2 storage primarily revolve around several key issues. Firstly, the inherently low adsorption capacity of physisorption methods, which are still far from meeting the densities required for commercial applications, limits their efficacy in energy-intensive applications with volume or weight restrictions. Secondly, thermal management challenges arise as H_2 adsorption and release are often accompanied by significant heat effects, which can lead to inefficiencies due to the need to overcome the heat of adsorption during H_2 release. Thirdly, the long-term stability and cycle life of materials mentioned above are critical concerns, as these materials can degrade structurally during repeated adsorption and release cycles, affecting performance and reliability. Moreover, the economic viability and scalability of using nanomaterials for physisorption pose significant barriers due to high projected production costs and technical challenges in scaling up manufacturing of target forms such as pellets, disks, and sheets. To achieve high storage capacities, it may be necessary to increase the surface area, improve the accessibility of pores, or introduce additional binding sites. However, practical applications face challenges, primarily the need for densification without compromising adsorptive performance besides the ones mentioned above. Given the extensive discussions on physisorption already prevalent in the literature,[49] we will focus only on highlighting a few recent breakthroughs.

One of the examples includes the use of densified HKUST-1 monoliths to achieve high volumetric and gravimetric H_2 storage capacities.[50] In this study, Madden, Chapman, and Fairen-Jimenez et al. present a novel approach by employing high-throughput screening to select the optimized MOFs for H_2 storage, specifically HKUST-1 (**Figure 2a**). This process was crucial in identifying an optimal structure that could be synthesized into densified monolithic forms ($_{\text{mono}}$MOFs) without losing adsorptive efficiency. The advanced synthesis technique developed involves a sol-gel process, allowing the formation of $_{\text{mono}}$MOFs that significantly enhance the practical application of H_2 storage. These $_{\text{mono}}$MOFs were able to achieve H_2 storage capacities of 46 g L^{-1} at 50 bar and 77 K. Remarkably, these structures require much lower operating pressures for H_2 release compared to traditional high-pressure gas storage methods, offering safer solutions for H_2 storage in fuel cell applications. Another example is the development of air-stable MOFs for H_2 storage at ambient conditions. For example, Islamoglu, Yildirim, and Farha et al. discuss the development and analysis of an air-stable Cu(I)-based MOF, referred to as NU-2100, synthesized using a *de novo* synthetic strategy.[51] This MOF shows high H_2 storage capacity under ambient conditions, leveraging a novel Cu/Zn precursor strategy where Zn catalyzes the formation of NU-2100 from an intermediate without becoming part of the final structure. The synthesized NU-2100 demonstrated one of the highest initial isosteric heats of adsorption noted among similar MOFs, with 32 kJ/mol (**Figure 2b**) and a good H_2 storage capability of 10.4 g/L under practical conditions (233 K/100 bar to 296 K/5 bar). Here, NU-2100's air stability is emphasized as a key attribute, contrasting with many Cu(I)-based MOFs that rapidly oxidize in air. The results indicate potent potential for NU-2100 in practical applications due to its air stability and effective H_2 adsorption characteristics, setting a foundation for further development of Cu(I)-MOFs for H_2 storage at ambient temperatures.

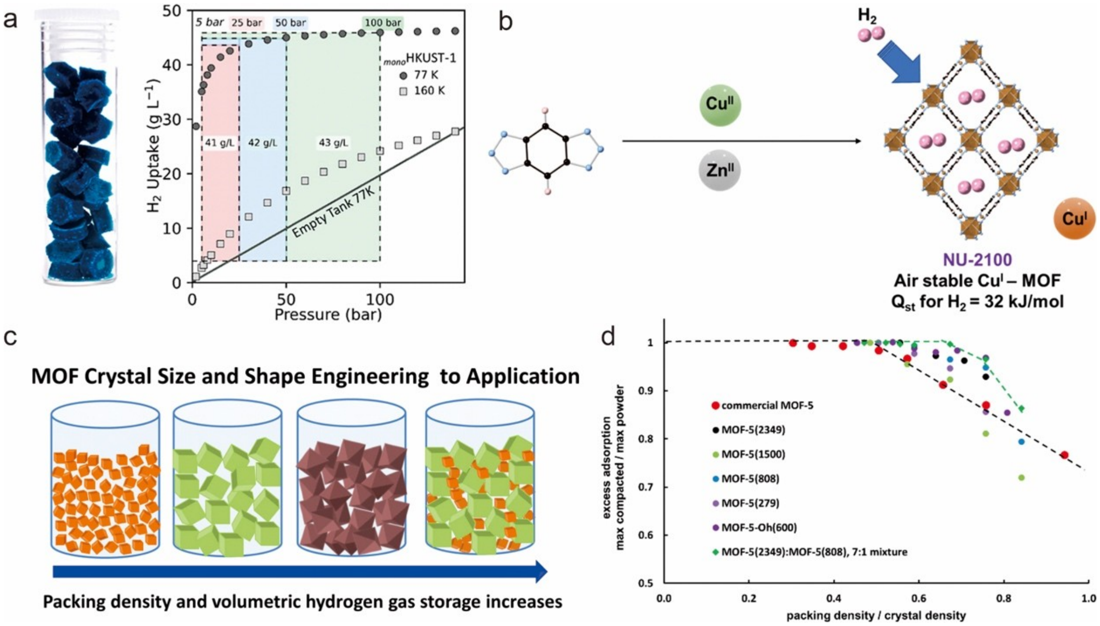

Figure 2. Densified HKUST-1 monoliths (a) and air-stable Cu(I)-based MOF (b) for H_2 storage. (c) Optimizing H_2 storage in MOF-5 through engineering of crystal morphology and control of crystal size. Reproduced with permission from ref. 50, 51, and 52 from the American Chemical Society, Copyright 2022, 2023, and 2021, respectively.

The optimization of H_2 storage in MOFs can also be achieved by engineering crystal morphology and controlling crystal size. For example, Suresh et al. specifically addresses the limitations of MOFs in achieving theoretical volumetric storage densities due to poor powder packing, as shown in **Figure 2c**.[52] By adjusting the engineering of crystal morphology and size, particularly for MOF-5, the team was able to substantially enhance volumetric H_2 storage performance. They demonstrated that both the crystal size and shape significantly influence the packing efficiency, which in turn impacts the volumetric H_2 storage capacity. The study also revealed that MOF packing efficiency is crucial for improving volumetric storage density in practical systems.

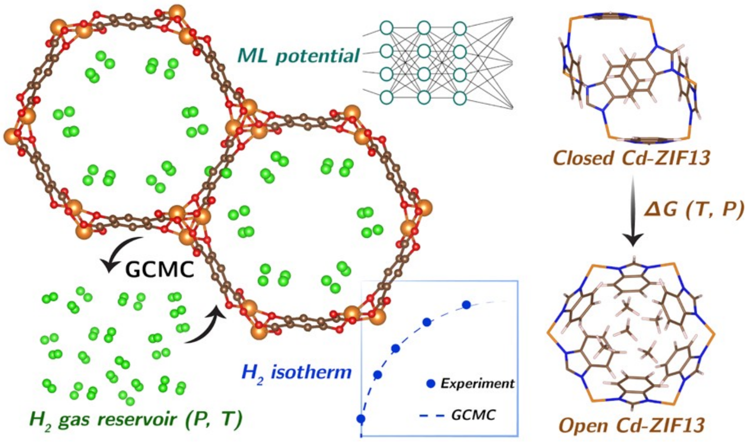

Figure 3. The use of Grand canonical Monte Carlo (GCMC) simulations to predict H2 adsorption isotherms to screen MOF-based physisorbents.

Theoretical modeling also shows promise in screening MOF-based physisorbents and identifying candidates that exhibit desired H_2 adsorption isotherms. Due to the nonpolar nature of H_2, not all areas on MOFs attract H_2 equally; only certain locations, like metal centers, exhibit relatively high ΔH^o. Once these sites are occupied, H_2 fills the remaining free void space, often necessitating significantly higher partial pressures. This heterogeneous gas-sorbent interaction leads to non-monotonic adsorption behavior, typically requiring the use of Grand canonical Monte Carlo (GCMC) simulations[53-55] to predict adsorption isotherms, as shown in **Figure 3**.

The accuracy of GCMC simulations heavily relies on the reliability of the force field describing gas-sorbent and gas-gas interactions. However, accurately predicting the weak interactions among H_2 and MOFs, especially with metal centers crucial for its differential enthalpy of adsorption at zero coverage, poses a challenge. In this regard, Head-Gorden et al. extensively benchmarked various density functionals for their performance in predicting H_2-metal and H_2-ligand interactions in MOFs. Once an appropriate density functional is selected and verified by experimental data on the differential enthalpy of adsorption obtained with microcalorimetry, it becomes feasible to parameterize force fields with improved reliability.[56, 57] Alternatively, training a machine-learning (ML) interatomic potential with density functional energetics is an option,[58] although the same density functional may not be simultaneously accurate for predicting both H_2-MOF and H_2- H_2 interactions. Furthermore, the transferability of ML potentials for other MOFs will greatly depend on the transferability of the density functional used. Having a force field or ML potential with balanced performance and uncertainty estimation across different MOFs will allow rapid screening of MOFs with desired H_2 adsorption profiles in the future.

While most porous materials primarily use physisorption for H_2 storage, a few undergo chemisorption following chemical modifications or treatments. For instance, Long et al.

discovered new chemisorption mechanisms at metal sites within porous frameworks, particularly focusing on CuI-MFU-4l[59]. Their findings revealed that the activation energy barrier for forming a precursor intermediate is linked to a structural change in the primary coordination sphere of Cu. This observation emphasizes the need for detailed studies to uncover such metastable intermediates, which are often overlooked in adsorptive processes. Employing *in situ* powder neutron diffraction experiments, the research provided crystallographic characterization of this intermediate. Further confirmation came from temperature-programmed desorption and DFT calculations. The change in the Cu^+ coordination environment, enhancing π-back bonding with H_2, suggests that chemisorption at these sites may not follow a direct pathway, highlighting the importance of kinetic analysis in developing advanced adsorbents. This study lays the groundwork for future research to identify similar intermediates in other chemisorption processes within porous materials. Another study by Liu et al. explores the development of a defective Mg-MOF-74 framework, termed de-MgMOF, for H_2 storage at above-ambient temperatures, using a Pt catalyst to enhance its capabilities.[60] The de-MgMOF is created by mildly annealing Mg-MOF-74, which introduces linker vacancies while preserving some crystal properties of the original framework. This results in unsaturated MgO_5 sites near these vacancies, exhibiting strong chemisorption interactions with H_2. With the aid of a small amount of Pt catalyst, de-MgMOF achieves a reversible H_2 storage capacity of 2.55 wt.% at 160°C and 81 bar pressure. The material also demonstrates rapid H_2 uptake/release, excellent cycling stability, and remains stable in natural storage conditions. This breakthrough also offers significant advancements in the practical application of MOFs for H_2 storage at temperatures near or higher than ambient, and modest pressures.

Nevertheless, despite their high surface areas, MOFs and other microporous structures typically have low reaction enthalpies for H_2 adsorption, generally ranging from 2 to 10 kJ/mol. This low binding energy is a significant limitation for room temperature applications because it means that H_2 is only weakly bound and can be released too easily at higher temperatures or lower pressures. To address this, chemical tuning of MOFs can be employed to enhance H_2 binding energetics. By incorporating metal ions or functional groups that can interact more strongly with H_2, the binding energy can be increased. For instance, introducing cations like Na^+, Li^+ into the structure of MOFs has been shown to increase the H_2 adsorption enthalpy to about 15-20 kJ/mol, thus enhancing the usable H_2 capacity at room temperature.

Distinctly different from MOFs, others novel materials like aluminum formate (ALF), composed of Al ions and formate anions linked through ionic and covalent bonds, forms a stable network that can also be used for efficient H_2 storage.[61] Its ReO_3-type structure indicates that it has a microporous structure, which enables it to physically adsorb H_2 within these pores. Evans, Yildirim, and Brown et al. demonstrate that ALF exhibits excellent H_2 adsorption at non-cryogenic temperatures (above 120 K) and moderate pressures (10 to 20 bar). Experimental methods, including gas isotherms, *in situ* neutron powder diffraction, and density functional theory (DFT) calculations, reveal the effective H_2 adsorption of ALF across a wide temperature range from 77 to 296 K. For instance, ALF shows an adsorption of approximately 11 g of H_2 per kg of ALF at about 120 K and 25 bar. The low raw material costs and straightforward synthesis make ALF an important emerging solution despite cooling requirements.

Building upon the application of nanotechnology to enhance physisorption techniques for solid-state H_2 storage at around room temperature when moving forward, we believe several innovative strategies will emerge that could not only augment current technologies but also pave the way for new research and application areas. For example, the development of smart nanomaterials with responsive properties could enable automatic regulation of H_2 adsorption and release under specific environmental stimuli, such as changes in temperature, pressure, or chemical surroundings. Recently, McGuirk et al. delves into enhancing H_2 storage using a multivariate approach MOFs.[62] The study focuses on a modified framework, specifically a derivative of CdIF-13, which is infused with a 2-methyl-5,6-difluorobenzimidazolate to adjust its adsorption threshold pressures effectively. This modification has resulted in a flexible framework that can switch from a nonporous to a porous structure upon reaching a certain pressure threshold, facilitating a step-shaped adsorption-desorption profile. This feature significantly enhances the usable H_2 capacity at comparatively mild pressure swings. The study also reports that this modified framework exhibits a usable H_2 capacity above 1 mass %, which represents 85-92% of its total capacity, at much lower pressures than typically required. The findings suggest that this approach can substantially reduce the energetic costs associated with H_2 storage, making it a promising technology for sustainable energy applications. Further development of flexible MOFs would benefit from deeper understanding of the mechanisms associated with adsorption-induced phase transformation, typically from closed to open states (as illustrated on the right of **Figure 3**). However, accurately modeling the phase transformation and its dependence on the partial pressure of the adsorbing gas species is not an easy task. Firstly, reliably probing the energy landscape associated with phase transformation necessitates the random phase approximation level of theory,[63, 64] which easily becomes computationally intractable for MOFs with relatively large pore sizes. Secondly, determining the pressure threshold of phase transformation requires explicit and dynamic modeling of condensed gas adsorption in MOFs[65] and appropriate thermodynamic models[66] to track the free energy profiles at finite temperatures. Despite progress made in these regards, an integrated fully first-principles approach that predictively recovers the isotherm of H_2 in a model flexible MOF awaits demonstration which necessitates collective effort from the community of computational MOF and adsorption. Such an achievement would allow subsequent engineering and systems analysis to begin to innovate on associated storage tank and thermal management designs.

Experimentalists could also consider developing thermosensitive MOFs that alter their pore structures upon reaching specific temperature thresholds around room temperature, thereby optimizing the dynamics of H_2 adsorption and release. Such materials could greatly enhance the overall efficiency and responsiveness of H_2 energy systems, providing rapid energy output during peak demand times or emergencies for the end user. Interface engineering and heterostructure design could further enhance material performance for H_2 storage. Moreover, creating synergies between different nanomaterials, such as introducing transition metals like Mg, Ni, Ti, or Cu into MOFs or incorporating carbon-based structures, can also lead to the development of novel composites. These composites combine the strengths of each component, such as high surface area and excellent chemical stability, can improve their H_2 adsorption thermodynamics.

Another challenge with MOFs is their poor heat transport properties. During the adsorption process, heat is released, and the inability of MOFs to effectively dissipate this heat can lead to localized heating. This heat accumulation can adversely affect the H_2 adsorption process, as increased temperatures can reduce the amount of H_2 that can be physiosorbed. In large-scale applications, this limitation can significantly impact efficiency, as managing heat becomes more challenging with larger volumes of stored H_2. Therefore, to mitigate these thermal management issues, a design incorporating MOFs with conductive carbon-based composites, where MOFs provide a high density of active sites and conductive carbon like graphene offers high electrical/thermal conductivity and mechanical stability, could significantly increase H_2 adsorption capacity while accelerating H_2 transfer rates, crucial for power systems. These composites can enhance the overall heat dissipation of the system, thereby maintaining a more uniform temperature profile and improving the efficiency of H_2 storage.

Additionally, research should also be integrated into the development of H_2 adsorbers by considering their life cycle, from synthesis to usage to recycling. For example, developing nanomaterials that can directly capture and store H_2, or gas that can later be converted into H_2 from industrial emissions, reduces environmental pollution and provides new pathways for the recycling and reuse of H_2 energy.

3.2 Chemisorption

In the context of H_2 storage, chemisorption involves the chemical integration of H_2 molecules onto a material surface, facilitating enhanced storage capacity compared to physisorption[67]. This mechanism widely exists in metal hydrides[68-75], intermetallic hydrides, liquid organic H_2 carriers[76, 77], and certain porous MOFs as discussed above. Notably, chemisorption processes usually require high activation energies for both adsorption and desorption due to strong interactions like valence forces in chemical compounds. The chemical bonds formed during chemisorption have substantial binding energies, sometimes exceeding 50 kJ/mol[68], necessitating thermal or catalytic activation to overcome the dissociation energy barrier. In this discussion, we focus on light metal hydrides and complex hydrides rather than simple metal and intermetallic hydrides due to their superior H_2 storage capacities and more favorable thermodynamic properties. Additionally, liquid organic H_2 carriers (LOHCs), which are typically non-metallic and often hydrocarbons, are not covered further here as they represent a distinct category separate from the solid-state based storage solutions discussed.

The chemisorption process involves the integration of H_2 atoms into the crystal lattice of a metal or alloy, leading to the formation of a new phase: a hydrogenated metal. The potential for high storage density makes metal hydrides particularly attractive for applications such as H_2-fueled vehicles and fuel cells. However, challenges remain with the rates of H_2 absorption and desorption, as well as the required operating conditions. Current research efforts aim to develop materials that provide considerable H_2 storage capacity through chemisorption while also offering favorable operational characteristics. Among which, strategies include developing nanostructured materials to increase surface area and reduce diffusion pathways, enhancing the dynamics of H_2 absorption and desorption, and designing novel materials with tailored chemistries [78].

3.2.1 Light Metal hydrides

Light metal hydrides, including MgH_2, sodium hydrides (NaH), and lithium hydrides (LiH), are recognized for their high H_2 storage capacity and functional properties such as heat resistance, vibration absorption, recyclability, and reversibility[74, 79, 80]. Each type of hydride presents unique properties and challenges. For instance, NaH can technically store a substantial amount of H_2 with weight percentage of 4.2% [81] but has a high reaction enthalpy, requiring significant heat to release stored H_2, which may hinder its practicality in applications needing quick H_2 release. LiH, offering an even higher H_2 content of 12.7%[82], faces similar thermal challenges and additionally poses safety risks due to its violent reaction with water and air, necessitating specialized handling and storage conditions. MgH_2 stands out due to its high energy density, providing a substantial H_2 capacity of 7.6 wt% and benefiting from both the low cost[83] and abundance of Mg [73]. Consequently, Mg-based hydrides have attracted considerable attention for their favorable properties and cost-effectiveness[84-86]. However, they also encounter challenges related to their thermodynamic and kinetic properties[72, 87], primarily due to the strong bonding between Mg and H_2, which requires high temperatures to decompose and results in slow absorption/desorption kinetics. In this section, we will focus on the potential and challenges of Mg-based hydrides.

Numerous research efforts have focused on improving the properties of Mg-based hydrides, particularly aiming to lower the desorption temperature and accelerate the re/dehydrogenation processes. These improvements can be achieved by modifying the hydride's microstructure with destabilizing elements and employing suitable catalysts to enhance kinetics. Techniques such as producing ultra-fine microstructures[85] and adding catalysts like transition metals[88], rare earth metals[89], and transition metal oxides[90] have been explored. Particle size reduction to the nanometer scale, significantly enhances the H_2 absorption/desorption properties of these alloys. For example, high-energy ball milling can not only reduce grain size of Mg and introduces numerous lattice defects but also allows for the synthesis of MgH_2 doped with catalytic additives[91]. The technique facilitates the creation of hydrides with desirable properties in a single step, maintaining their gravimetric H_2 storage capacity.

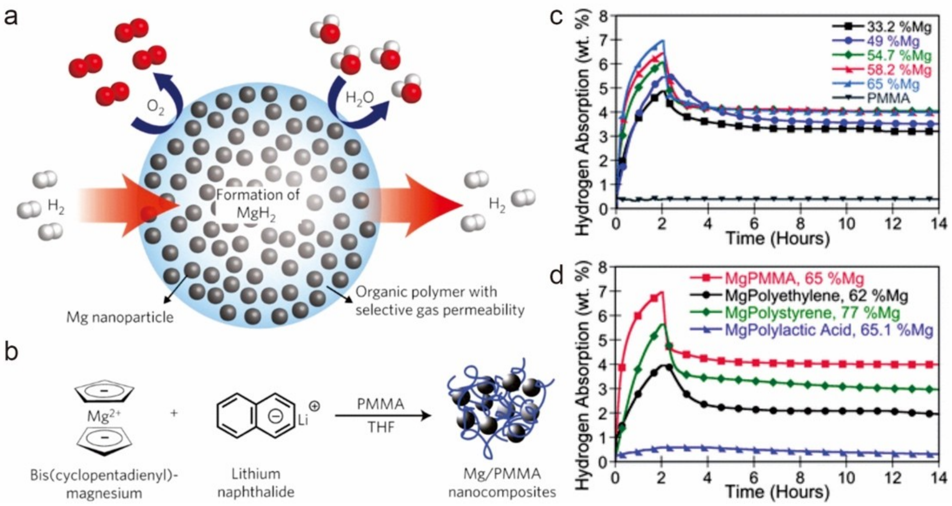

Figure 4. Mg in a gas-barrier polymer matrix. (a) Schematic of H_2 storage composite material: high-capacity Mg are encapsulated by a selectively gas-permeable PMMA polymer. Reproduced with permission from ref. 94 from Nature publishing group, Copyright 2011. (b), Synthetic approach to formation of Mg/PMMA nanocomposites. Reprinted with permission from reference X. (c) H_2 absorption (200 °C, 30 bar H_2) and desorption (300 °C, 0 bar H_2) of Mg–polymer nanocomposites containing 33.2, 49, 54.7, 58.2 and 65 wt% Mg, and Mg–polymer nanocomposites composed of PMMA, PE, PS, and PLA. Reproduced with permission from ref. 99 from the Royal Society of Chemistry, Copyright 2017.

Integrating nanomaterials into H_2 storage technologies also presents challenges. These include ensuring stability over many cycles of H_2 absorption and desorption, preventing agglomeration of nanoparticles, and scaling up the production of nanomaterials in a cost-effective manner. Over the past decade, the Urban group reported many important innovations orbiting around the central concept of using nano-sized Mg-based metal hydrides for H_2 storage[78, 92-98]. In 2011, we introduced a novel air-stable Mg nanocomposite, which provides rapid and high capacity H_2 storage without the need for heavy-metal catalysts[94]. Central to this technology are Mg nanocrystals embedded in a gas and moisture barrier poly(methyl methacrylate) (PMMA) matrix (**Figure 4a-b**). This matrix prevents oxidation while enabling efficient H_2 absorption and release. This innovation immediately enabled the usage of nanomaterials for pragmatic applications and let to collaborations with companies to further develop the technology. Importantly, the flexible matrix also accommodates the ca. 33% lattice expansion upon sorption and release of hydrogen in the process of forming the metal hydride MgH_2. This preliminary breakthrough directly synthesized nanocomposites at room temperature through a one-pot reduction reaction involving an organometallic Mg^{2+} precursor in a PMMA environment. This method achieves H_2 storage capacities of up to 6 wt% for Mg and 4 wt% for the composite, with absorption occurring in less than 30 minutes at 200°C (**Figure 4c**).[99] Notably, the nanostructuring of Mg within the composites ensures rapid storage kinetics without costly catalysts. This technique addresses a significant challenge in H_2 storage—balancing the need for strong H_2 absorption for stable storage and weak absorption for easy release. Traditional metal hydrides, though effective at storing H_2, often require high release temperatures, which lead to low energy efficiency. In contrast, the nanostructured Mg promotes enhanced kinetics by shortening diffusion paths for H_2 and reducing the thickness of the hydride layer that forms during absorption.

We further explored how varying the metal-polymer interfaces within a Mg-polymer nanocomposite affects the air stability of the composite and their H_2 absorption characteristics.[93] Remarkably, it was found that decreasing the amount of polymer in the composite increases both the air stability of Mg and the H_2 sorption capacity (~6.95 wt%). This improvement is attributed to an increase in the tortuosity of gas molecule paths and enhanced interfacial structure-templating regions that scale with the Mg content. These features effectively hinder polymer chain motion and enhance the composite's functional properties. We also investigated the H_2 storage capabilities of Mg-polymer nanocomposites utilizing various polymers, including PMMA, polyethylene (PE), polystyrene (PS), and polylactic acid (PLA), as can be seen in **Figure 4d**. Among which, PMMA composites exhibited the highest H_2 storage efficiency, due to effective gas barrier properties and optimal interfacial interactions with Mg nanocrystals. In contrast, PLA composites underperformed because of irregular Mg crystal growth and slight oxidation issues, attributed to the synthetic method which added the polymer late in the process. PE and PS showed decent performance but did not match PMMA's effectiveness. This study highlights the significant role of polymer selection in enhancing the functionality of Mg-based nanocomposites for H_2 storage.

We further pushed this functional scaffolding concept to the ultimate limit by integrating Mg particles on sheets of atomically thin reduced graphene oxide (rGO). This was inspired by research in the membrane's community showing excellent discrimination of rGO for H_2 vs. many other gas pairs in separations applications. This concept offered several advantages over Mg-polymer hybrid materials for H_2 storage. Firstly, atomically thin layers of rGO minimize inactive mass while providing superior environmental protection by effectively blocking oxygen and moisture. This enhances the stability and longevity of Mg for H_2 storage. Secondly, rGO provides exceptional stability under environmental exposure, allowing Mg nanocrystals to retain their zero-valent state and reactivity without significant degradation. In contrast, polymers may not offer the same level of protection against oxidation or moisture, potentially leading to quicker degradation and reduced efficacy of the storage material. Thirdly, unlike polymers, rGO not only acts as a protective barrier but also catalytically enhances the kinetics of H_2 absorption and desorption, critical for the practical application of H_2 storage materials as it allows for quicker charging and discharging cycles. Additionally, the high Young's modulus of rGO helps maintain the structural integrity of the composite during the expansion and contraction cycles associated with H_2 sorption and desorption, a feature polymer may lack, potentially leading to mechanical fracture or deformation. While we have not yet quantified the thermal conductivity, simple materials considerations support the notion that rGO should have better thermal properties than prior polymers used, another potential benefit in managing the heat of absorption/release inherent to the use of metal hydrides.

In practice, the rGO/Mg nanocrystal multilaminates worked well as functional storage materials, as seen in **Figure 5 a-c**.[100] This composite demonstrates a high H_2 storage capacity of 6.5 wt% (this storage capacity *includes* the mass of the rGO, and is close to the theoretical maximum of Mg itself) and excellent environmental stability, making it a promising candidate for solid-state H_2 storage applications. This innovative use of rGO in the composite addresses major challenges previously faced by metal hydrides, such as oxidative instability and poor kinetics. Wan et al. further highlights the pivotal role of an atomically thin interfacial suboxide layer in enhancing the H_2 storage performance of Mg nanoparticles encapsulated in rGO.[101] The research identifies that an ultra-thin layer of MgO forms at the nanoparticle-rGO interface, which contrary to conventional belief, does not hinder but facilitates H_2 storage (**Figure 5d**). This interfacial suboxide layer is crucial because it enables H_2 molecules to dissociate similarly to how they would on pristine Mg metal surfaces. The interaction between the rGO and Mg nanoparticles is strengthened by this suboxide layer, enhancing the mechanical and chemical stability of the composite, which is vital for operational longevity and efficiency. DFT calculations were used to investigate this phenomenon, focusing on the H_2 adsorption and dissociation mechanisms on these novel nanostructures. The results reveal that this suboxide layer allows H_2 dissociation with an energy penalty comparable to that on a pristine Mg surface, proving that the initial assumptions about the detrimental effects of MgO on H_2 storage were misplaced. This breakthrough underscores a significant advancement in H_2 storage technology, showcasing that the nanoengineering of interfacial layers within composites can drastically alter and improve functional properties.

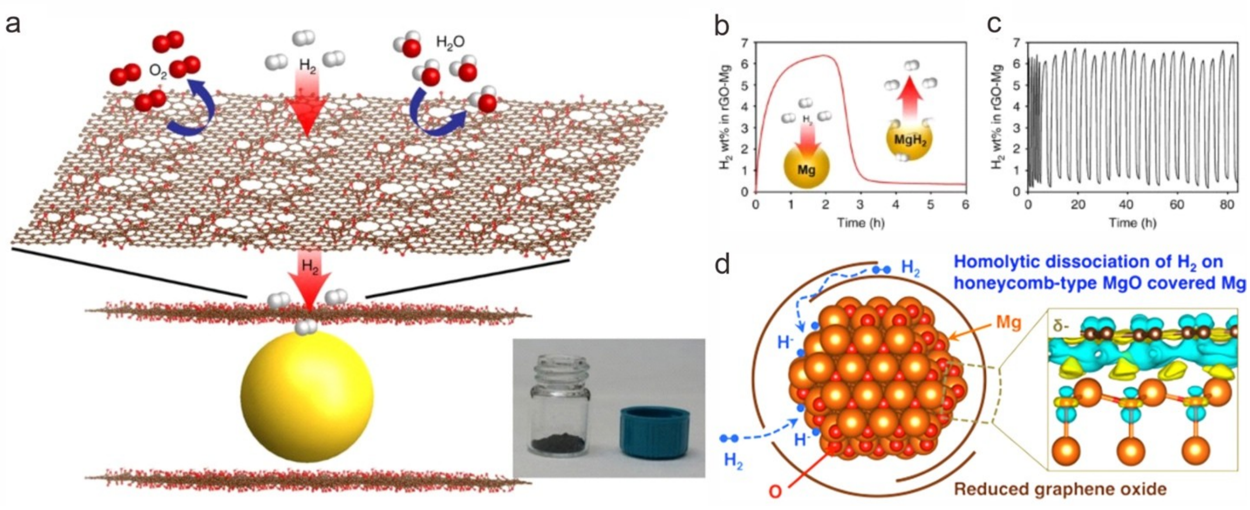

Figure 5. (a) Illustrations depicting the structure of rGO-Mg nanolaminates where rGO layers prevent O_2 and H2O from penetrating, while allowing the diffusion of H_2 (b) and (c) H_2 absorption/desorption characterization of rGO-Mg

multilaminate. Reproduced with permission from ref. 100 from Nature publishing group, Copyright 2016. (d) Illustrations of homolytic dissociation of H_2 on honeycomb-type MgO covered Mg. Reproduced with permission from ref. 101 from the American Chemical Society, Copyright 2017.

Furthermore, in the realm of H_2 storage, the selection and integration of metal dopants into Mg nanocomposites also play a crucial role in enhancing their performance. Based on previous study in the Urban group,[92] metal dopants such as Ni, Ti, and Co significantly influence the H_2 storage properties by modifying the kinetics and thermodynamics of the Mg-based systems (**Figure 6a**). Each metal offers distinct benefits and affects the storage capacity and release rates differently, making their study essential for optimizing H_2 storage technologies (**Figure 6b**). For example, we found out that Ti, when used as a dopant, primarily enhances the H_2 absorption rate, in which, it acts as a catalyst that facilitates the rapid dissociation of H_2 molecules at the material's surface, which accelerates the overall H_2 uptake. However, Ti does not significantly improve the desorption kinetics, which is a critical factor for the practical use of H_2 as a fuel, where both fast charging and discharging are required. Co, similar to Ti, improves the absorption kinetics and has a strong catalytic effect that speeds up the initial H_2 uptake but, like Ti, does not markedly enhance the H_2 release rates. This limitation restricts the overall effectiveness of Co-doped composites in applications requiring quick cycling between H_2 storage and release.

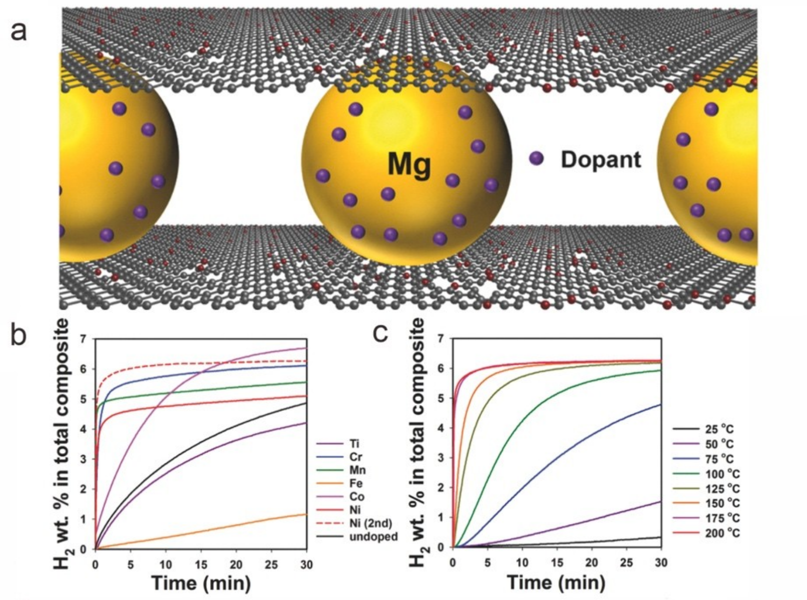

		ΔH (kJ/mol)	ΔS (J/mol·K)
Absorption	**bulk Mg**	-74.8	-135
	rGO-Mg	-65.6	-122.1
	Ni-doped rGO-Mg	-63.9	-119.4
Desorption	**bulk Mg**	76.3	130
	rGO-Mg	69.4	126.3
	Ni-doped rGO-Mg	66.9	122.0

Figure 6. (a) Illustration describing Mg nanocrystals encapsulated by rGO layers with transition metal dopants (transition metal doped rGO–Mg). (b) H_2 absorption behaviors of a series of 3D transition metal doped rGO–Mg composites at 15 bar of H_2 and 200 °C in comparison with undoped rGO–Mg; red solid and dashed line represent the absorption of the first and the second H_2 sorption cycles for Ni-doped rGO–Mg, respectively. (c) H_2 absorption at 15 bar of H_2 and b) desorption at 0 bar at different temperatures for Ni-doped Mg crystals embedded in rGO layers (Ni-doped rGO–Mg); the capacity is based on the entire composite weight. (d) Thermodynamic parameters of rGO–Mg and Ni-doped rGO–Mg composite. Reproduced with permission from ref. 92 from the Wiley, Copyright 2017.

In contrast, Ni-doped Mg-rGO composites stand out among dopants for their ability to catalytically activate both the H_2 absorption and desorption processes, demonstrating remarkable kinetic improvements. Specifically, the H_2 absorption capacity reached 6.5 wt% at 200°C, with 90% of this capacity achieved within just 2.5 minutes (**Figure 6c**). This is a significant enhancement over typical performance metrics for solid-state H_2 storage materials under similar conditions. The desorption process was equally efficient, with 90% of H_2 being released within 4.6 minutes at 300°C. This enhanced kinetic performance is due to the catalytic activity of Ni, which effectively reduces the energy barriers associated with H_2 sorption. For Ni-doped Mg-rGO, the activation energy for H_2 absorption is significantly lowered compared to other metal-doped systems (**Figure 6d**), suggesting a more effective catalytic role of Ni in facilitating rapid H_2 dynamics at the nanoscale. These kinetic enhancements are critical for practical H_2 storage applications, providing faster charging and discharging cycles which are essential for operational efficiency in real-world applications.

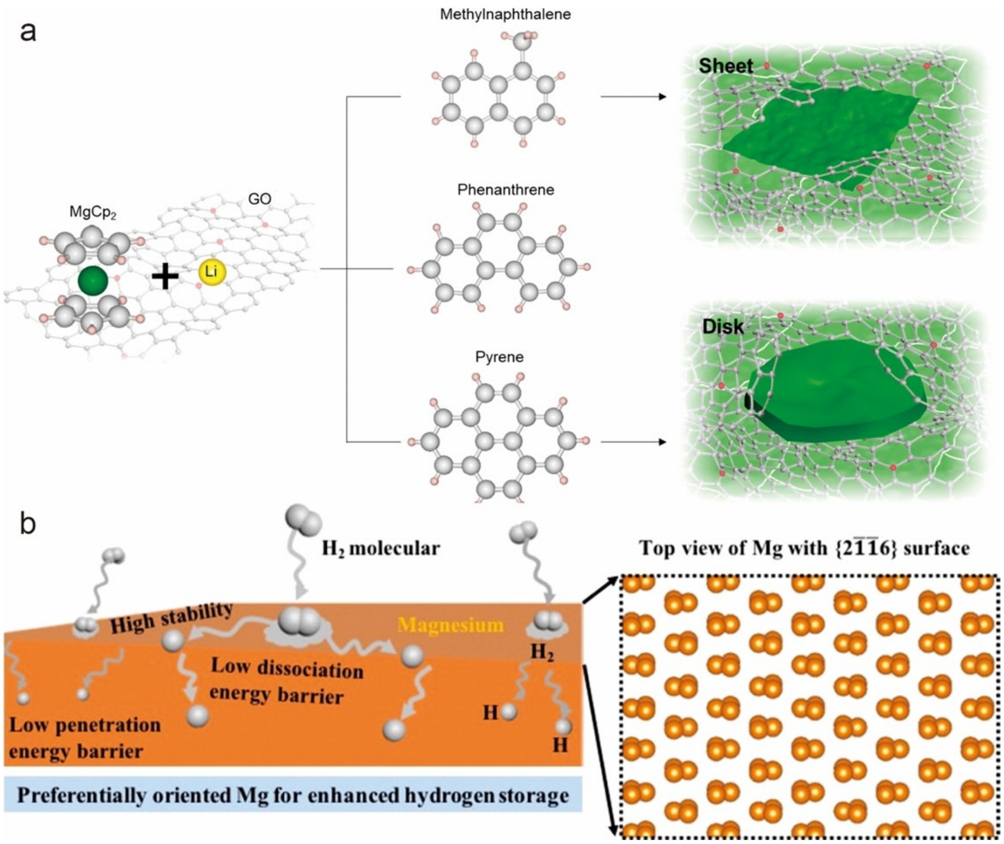

Figure 7. (a) Synthetic approach to the formation of magnesium particles using different reducing agents based on $MgCl_2$ precusors. (b) Preferentially oriented Mg with high index $\{2\acute{1}\acute{1}6\}$ planes and rGO hybrids for H_2 storage. Reproduced with permission from ref. 78 from the American Chemical Society, Copyright 2022.

Previous investigations in the Urban group had also highlighted the impact of Mg crystal orientation on H_2 storage performance, emphasizing how different exposed Mg facets influence H_2 adsorption and desorption. For example, we synthesized Mg particles with specific crystal facets, namely the close-packed {0001} and the high-index $\{2\acute{1}\acute{1}6\}$ planes, on rGO.[78] This differentiation in crystal facets had a significant effect on H_2 storage capabilities: Particles with a preferentially exposed high index $\{2\acute{1}\acute{1}6\}$ crystal surface exhibited a markedly increased H_2 absorption capacity up to 6.2 wt% compared to systems with no preferential orientation, which showed lower performance of 5.1 wt% within the first two hours (**Figure 7a**). We believe the $\{2\acute{1}\acute{1}6\}$ surface provided lower H_2 dissociation energy barriers and more stable H_2 atom retention compared to the {0001} basal plane, contributing to enhanced H_2 sorption properties (**Figure 7b**). First-principles calculations supported the experimental findings, revealing that the $\{2\acute{1}\acute{1}6\}$ surface had a much lower H_2 penetration energy barrier due to its reduced surface atom packing density, significantly enhancing the hydrogenation kinetics. This study underscores the critical role of Mg crystal orientation in optimizing H_2 storage performance, suggesting that controlled manipulation of exposed crystal facets can also significantly enhance the efficiency of H_2 storage materials.

Finally, beyond rGO, the strategic design of edge-functional groups in graphene derivatives can also serve as a general approach for both encapsulating and catalyzing H_2 storage in simple metal or complex metal nanocrystals. For example, our previous study confirmed the enhancement of H_2 storage capabilities using edge-functionalized graphene nanoribbon (GNR)-encapsulated Mg nanocrystals.[97] The study demonstrates that GNRs can be edge-functionalized with various groups to tune the dehydrogenation kinetics effectively. By employing different edge-functional groups on the GNRs, the study compares their effects on cycling performance. The kinetic analysis, supported by first-principles calculations, suggests that these functional groups help reduce kinetic barriers for H_2 reactions at the GNR-Mg interfaces by stabilizing surface defects, thereby enhancing the H_2 storage capacity and stability of the material. One of the key findings is that the GNR-Mg composite exhibited a higher H_2 storage capacity of 7.1 wt% based on the total composite, superior to current alternatives, while also demonstrating enhanced long-term air stability. We note that many H_2 storage articles unfortunately mislead by not including the mass of the composite in the overall storage density figures reported; this makes apples-to-apples comparisons very difficult in the literature.

In sum, light metal hydrides represent a cornerstone in the field of solid-state H_2 storage, offering high H_2 densities. Over the past decade, the Urban group has made significant contributions to H_2

storage technology, especially in advancing chemisorption mechanisms. The team developed nanosized Mg-based nanocomposite materials, initially focusing on encapsulating magnesium nanocrystals within polymers like PMMA, creating air-stable composites. These composites could achieve up to 6% H_2 storage capacity within 30 minutes at 200°C. Subsequently, the polymers were replaced with rGO, and the resulting rGO/Mg nanolaminate composites demonstrated a 6.5% H_2 storage capacity and excellent environmental stability. Furthermore, the Urban group improved the H_2 adsorption and desorption kinetics of these storage materials by doping them with metals such as Ni, which significantly enhanced the rate of H_2 uptake and release, meeting the needs of practical applications. The group also explored crystal orientation engineering, discovering that specific crystal face orientations, like the high index planes, could significantly enhance H_2 adsorption capabilities. Additionally, using $MgCl_2$ as a source of magnesium provided an effective way to reduce the costs associated with H_2 storage technology. It is important to note that these advancements pertain solely to the material level and do not account for the additional weight of the storage tanks. Nevertheless, we believe these studies could push forward the performance of H_2 storage materials and laid a foundation for the application of nanotechnology in the field of solid-state H_2 storage.

3.2.2 Complex metal hydrides

Light metal hydrides are typically characterized by their relatively straightforward hydride formations and moderate H_2 storage capacities. In contrast, complex metal hydrides, involve more complex structures and bonding, often resulting in higher H_2 capacities and different thermodynamic and kinetic properties. This complexity can provide advantages in certain applications, where specific release temperatures and absorption pressures are crucial. Normally, these complex metal hydrides are composed of a metal cation, such as Li, Na, or Al, linked to complex anionic hydrides like alanates $[AlH_4]^-$, amides $[NH_2]^-$, imides, and borohydrides $[BH_4]^-$. In these materials, H_2 atoms are often tetrahedrally coordinated around the metal center. The high H_2 density of these hydrides makes them particularly appealing for applications that require compact and efficient energy storage solutions. Among them, alanates and $[BH_4]^-$ are of specific interest due to their lightweight properties and their capacity to host a significant number of H_2 atoms per metal atom[102]. However, these compounds exhibit different chemical behaviors: $[AlH_4]^-$, noted for their high H_2 storage capacities, typically release H_2 in a two-step process process[103], whereas $[BH_4]^-$, like $LiBH_4$ and $NaBH_4$, are recognized for their stability, decomposing only at higher temperature and showing limited reversibility under similar conditions. Furthermore, complex Al-based hydrides such as $NaAlH_4$, $KAlH_4$, and Na_3AlH_6 can be decomposed at elevated temperatures and rehydrogenated under technologically relevant conditions using catalysts. The practical application of these materials often faces challenges related to the conditions required for H_2 release and absorption, including specific pressures and temperatures, as well as the need for improved kinetic properties to facilitate rapid H_2 cycling.

When designing complex metal hydrides for efficient H_2 storage, the first thing to consider is the morphological context of these metal hydrides. Kang and Wood et al. explore the stability of complex metal hydrides influenced by their morphology, using first-principles calculations to understand the energetics of these materials during H_2 storage processes, as can be seen in **Figure 8a-b**.[104] They suggest that optimizing the morphology of metal hydrides could lead to better control of H_2 storage properties, such as improving the reversibility of H_2 absorption and desorption, thus enhancing the practical application of these materials in energy storage systems. The team particularly focuses on how the morphological evolution from dispersed molecules, through clustered molecular chains, to condensed-phase crystals affect the reaction pathways and stability of complex metal hydrides. By examining a range of complex light metal hydrides including sodium aluminum hydride ($NaAlH_4$), lithium amide ($LiNH_2$), and magnesium borohydride ($Mg(BH_4)_2$), among others, they found out that these hydrides exhibit various morphological stages that significantly impact their (de)hydrogenation kinetics and reversibility. Specifically, it was found that dispersed molecular forms can stabilize under certain conditions that are unfavorable in more condensed phases. The study highlights discrepancies often observed between experimental methods, which may miss non-crystalline intermediates, and nuclear magnetic resonance, which can detect a wider range of molecular environments. This detailed analysis provides insights into the energetics across different morphologies, showing that the stability and formation energies of intermediates vary, influencing how these materials behave in solid-state H_2 storage applications.

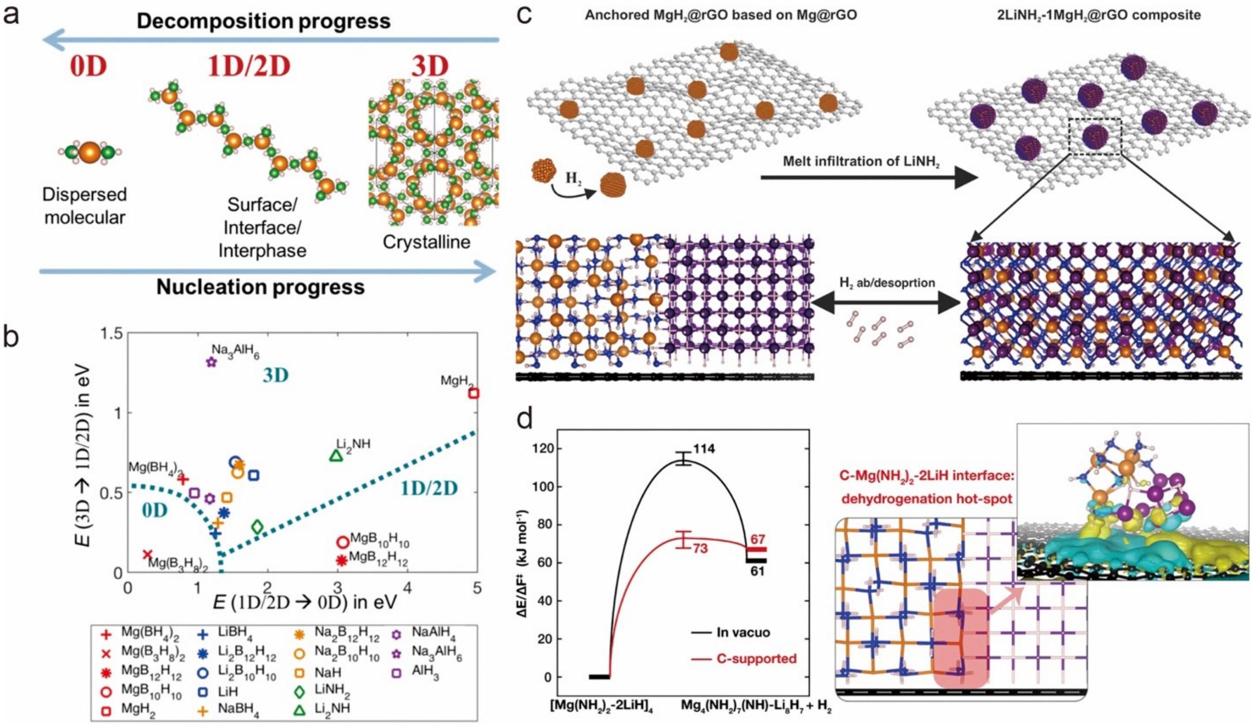

Figure 8. (a) Schematic of 0D, 1D/2D, and 3D models and their physical morphological interpretation. Phase nucleation follows an increase in dimension, whereas phase decomposition follows a decrease in dimension. (b)

Morphology-dependent metastability map for all tested H_2 containing compounds, plotted according to thermodynamic driving forces for 3D-to-1D/2D and 1D/2D-to-0D interconversion. Reproduced with permission from ref. 104 from the Wiley, Copyright 2019. (c) Schematic diagram of the fabrication process of $Li_2Mg(NH)_2$@rGO composite. (d) Reaction energies (ΔE) and free energy barriers ($\Delta F^{\ddagger}$) for the interfacial dehydrogenation of 2LiH-$Mg(NH_2)_2$ cluster with and without carbon support. Color scheme for different elements: black-C, orange-Mg, purple-Li, blue-N, pink-H. Color scheme for isosurfaces: yellow-charge accumulation, cyan-charge depletion. Reproduced with permission from ref. 105 from the Wiley, Copyright 2023.

Experimentally, the Urban group has successfully achieved nanoconfinement of $Li_2Mg(NH)_2$@rGO within the composite through melt infiltration, which significantly improves H_2 storage performance, as can be seen in **Figure 8c**.[105] This method not only facilitates efficient contact but also prevents the aggregation of active materials during the cycling process, thereby maintaining stability and enhancing performance through sustained close contact at the nanoscale. Specifically, this study demonstrates that incorporating rGO not only mitigates particle aggregation but also catalyzes H_2 bond cleavage at the Mg-amide/Li hydride interface, creating local dehydrogenation hotspots that significantly enhance the kinetics of H_2 release compared to bulk materials (**Figure 8d**). The composite displays a reversible H_2 storage capacity of 4.42 wt%, with no degradation observed after multiple cycles, underscoring the effectiveness of the nanostructured approach. Furthermore, the role of rGO is pivotal in this composite as it acts as a protective barrier that preserves the structural integrity and functional properties of the material under cycling conditions, illustrating its critical contribution to the improved performance of the composite.

Moreover, Stavila and Allendorf et al. also highlight the innovative approach of stabilizing alane (AlH_3) within covalent triazine frameworks (CTFs) to enhance reversible H_2 storage.[106] By embedding alane into nanoporous bipyridine-functionalized CTFs, the study demonstrates that H_2 can be desorbed from AlH_3 at significantly lower pressures and temperatures than previously achievable with bulk materials. Specifically, AlH_3 within CTFs can release H_2 at temperatures between 95°C and 154°C and reabsorb it under 700 bar of pressure, which is more than ten times lower than the 7000 bar typically required for rehydrogenating bulk Al. The nanoconfinement provided by the CTFs, with their structured and electron-donating sites, facilitates this process by altering the electronic environment of the alane, effectively lowering the activation energy for H_2 desorption and absorption. This approach also showcases a significant shift in handling the thermodynamic and kinetic challenges of complex metal hydrides in H_2 storage, leveraging the controlled environment of nanoconfinement to achieve improved performance metrics in H_2 storage technology. The same group also investigated H_2 storage in ultrathin MgB_2 multilayers produced through high-energy ball milling, emphasizing the significant role of nanoconfinement.[107] By exfoliating MgB_2 into nanosheets with a thickness of approximately 3-4 nm, the research showcases an enhanced hydrogenation capacity. Specifically, these multilayers achieve a H_2 storage capacity of 5.1 wt% under conditions of 700 bar pressure and 330°C, which is notably higher than the capacity observed in bulk MgB_2 under the same conditions (nearly 50 times greater). This improvement is attributed to the increased surface area and the creation of defective sites that facilitate more effective H_2 uptake and release. Additionally, the study notes that these nanosheets can be hydrogenated at significantly lower pressures and temperatures compared to bulk MgB_2, highlighting the advantages of nanostructuring in overcoming kinetic and thermodynamic barriers in H_2 storage technologies.

So far, the deployment of metal hydrides (both light metal hydrides and complex metal hydrides) in H_2 storage has reached a crucial juncture, hindered by traditional challenges such as kinetic limitations, thermodynamic stability, and reversibility, and novel ones such as material manufacturing at scale and heat management. To overcome these barriers and address both inherent material limitations and system-level integration challenges, the future of metal hydrides in H_2 storage is not limited to incremental improvements but requires a paradigm shift towards innovative sustainable materials, advanced manufacturing processes, and system integration. On one hand, future work could further explore the integration of single-atom catalysts to enhance the slow hydrogen-desorption kinetics. For example, recently, Huang et al. investigated the use of a single-atom Ni catalyst supported on TiO_2 to improve the H_2 storage capabilities of MgH_2.[108] The study demonstrates that a single-atom Ni-loaded TiO_2 can significantly enhancing hydrogen storage performance by lowering the onset dehydrogenation temperature of MgH_2 to 200°C and facilitating rapid rates of H_2 release and absorption. The optimized catalyst, 15wt%-$Ni_{0.034}$@TiO_2, achieved a H_2 release of 4.6 wt% within 5 minutes and an absorption of 6.53 wt% within 10 seconds at 300°C. This catalyst maintains high catalytic activity and stability even after 100 cycles of hydrogenation and dehydrogenation, with a capacity retention rate of 97.26%. The exceptional performance is attributed to the efficient electron transfer enabled by the single-atom Ni and the presence of oxygen vacancies and multivalent titanium ions in the TiO_2 support. This breakthrough not only offers a practical H_2 storage solution but also extends the application of single-atom catalysis in high-temperature solid-state reactions.

Additionally, as a new category, the integration of medium-entropy alloy (MEAs) or high-entropy alloys (HEAs) in solid-state H_2 storage presents an innovative avenue for exploration. These alloys, known for their exceptional mechanical properties and thermal stability, could potentially revolutionize H_2 storage capacities and release kinetics due to their unique compositional complexity. Recently, Balcerzak et al. explore the H_2 storage properties of a ScYNdGd medium-entropy alloy, demonstrating a significant capacity of 2.5 H/M (M stands for the metal atom), with hydrogenation performed under mild conditions at temperatures not exceeding 300°C and pressures up to 35 bar.[109] The alloy uniquely maintains a single-phase face-centered cubic structure throughout the hydrogenation process without any phase transformation, which contributes to its robust stability and reusability across more than 100 cycles. The reversible H_2 adsorption and desorption are characterized by rapid kinetics, with an absorption rate of 6.53 wt% within 10 seconds and a release of 4.6 wt% within 5 minutes at 300°C, evidencing efficient performance. The studies also provide insights into the H_2 desorption mechanism, where H_2 is released in two steps: initially from octahedral sites at lower temperatures and subsequently from tetrahedral sites at higher temperatures. This research sets a benchmark for future developments in H_2 storage technologies. Parallel theoretical modeling efforts are also crucial for advancing the fundamental understanding of H_2 storage in MEAs and HEAs. In these materials, atomic arrangements may be amorphous and, at most, exhibit only short-range order, significantly influenced by temperature. Exploring this configurational space computationally is a challenging task, with the insertion of H and its potential distribution at high loading adding another layer of complexity. However, recent advancements in integrating ML interatomic potentials and Monte Carlo simulations offer promising solutions to this computational challenge.[110] Future developments in metal hydrides should exploit computational materials science to predict and identify novel hydride compositions with optimized properties for target operation cycles where release pressure may influence material selection..

High-throughput screening, combined with ML algorithms, can identify patterns, and predict the behavior of hydride materials under various conditions, significantly reducing the time and cost associated with experimental trials. This approach could unveil new classes of lightweight hydrides with tailored thermodynamics profiles and enhanced reversibility. Advancing beyond conventional doping, molecular engineering can precisely control the microstructural features of hydrides at the atomic level. This involves manipulating the electronic and crystallographic structure to create specific sites for rapid H_2 uptake and release. Recently, Witman and Vitalie et al., explore a novel approach in the discovery of HEAs for H_2 storage using ML models, as can be seen in **Figure 9 and Figure 10**.[111] The research emphasizes the use of gradient boosting tree (GBT) models to predict the stability and hydrogen storage capacity of various HEA compositions rapidly. By leveraging ML, the team efficiently narrows down potential HEA candidates from a large dataset, which are then experimentally synthesized and tested to validate the predictions. Significant findings include the identification of new HEA hydrides that demonstrate improved H_2 storage capabilities. For instance, they detailed the synthesis and characterization of novel hydrides that show a 70× increase in equilibrium pressure and a 20 kJ/mol decrease in desorption enthalpy relative to benchmark HEA hydride $TiVZrNbHfH_x$. These advancements highlight the potential of integrating ML models into the material discovery process, offering a more streamlined and effective pathway to develop materials with tailored properties for H_2 storage.[112-114] Nevertheless, it is also important to note a significant challenging: while ML models can interpolate between pressure-composition-temperature (PCT) curves to understand how a single metal hydride performs under different temperature and pressure conditions, there may not be enough data available to effectively utilize ML for metal hydride presently. In fact, we believe it may be more appropriate in the near-future to consider implementing this ML approach for sorbents, as recent work with extensive sorbent databases is emerging rapidly.[112-114]

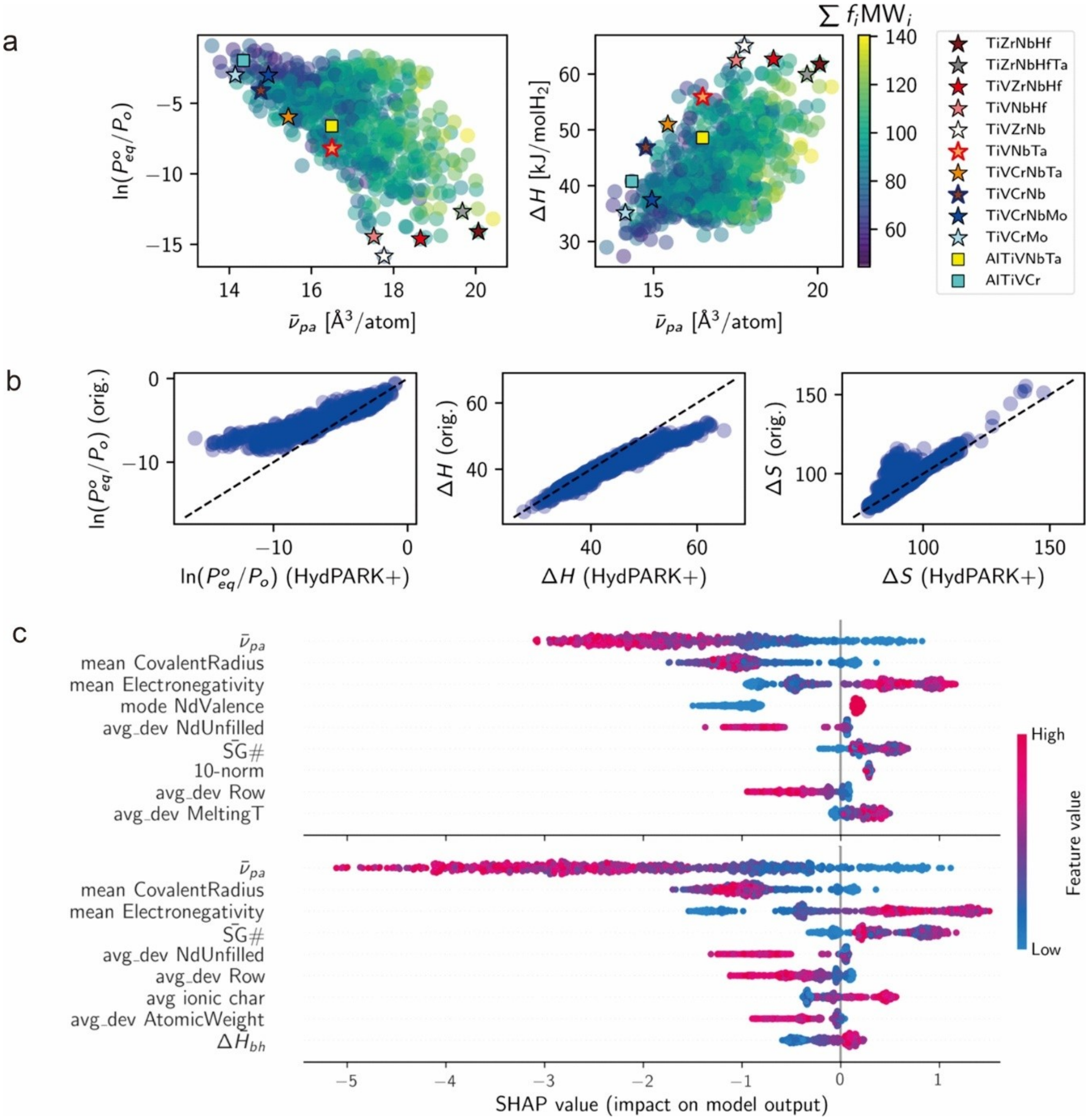

Figure 9. (a) ML-predicted $\ln(P_{eq}^{o}/P_{o})$ and ΔH vs $\bar{\nu}_{pa}$ for the rHEA data set. Stars represent materials previously synthesized and tested for H_2 uptake, while squares represent new candidates identified in this work. (b) Parity plots between rHEA thermodynamic predictions when using a model trained on the original HydPARK data set vs the HydPARK+ data set (dashed black line corresponds to $y = x$). Enthalpy change, ΔH, is in units of [kJ/molH$_2$] and entropy change, ΔS, is in units of [J/(molH$_2$·K)]. (c) SHAP values for $\ln(P_{eq}^{o}/P_{o})$ predictions on the rHEA data set for models trained on the original HydPARK (top) and HydPARK+ (bottom) data sets. Reproduced with permission from ref. 111 from the American Chemical Society, Copyright 2021.

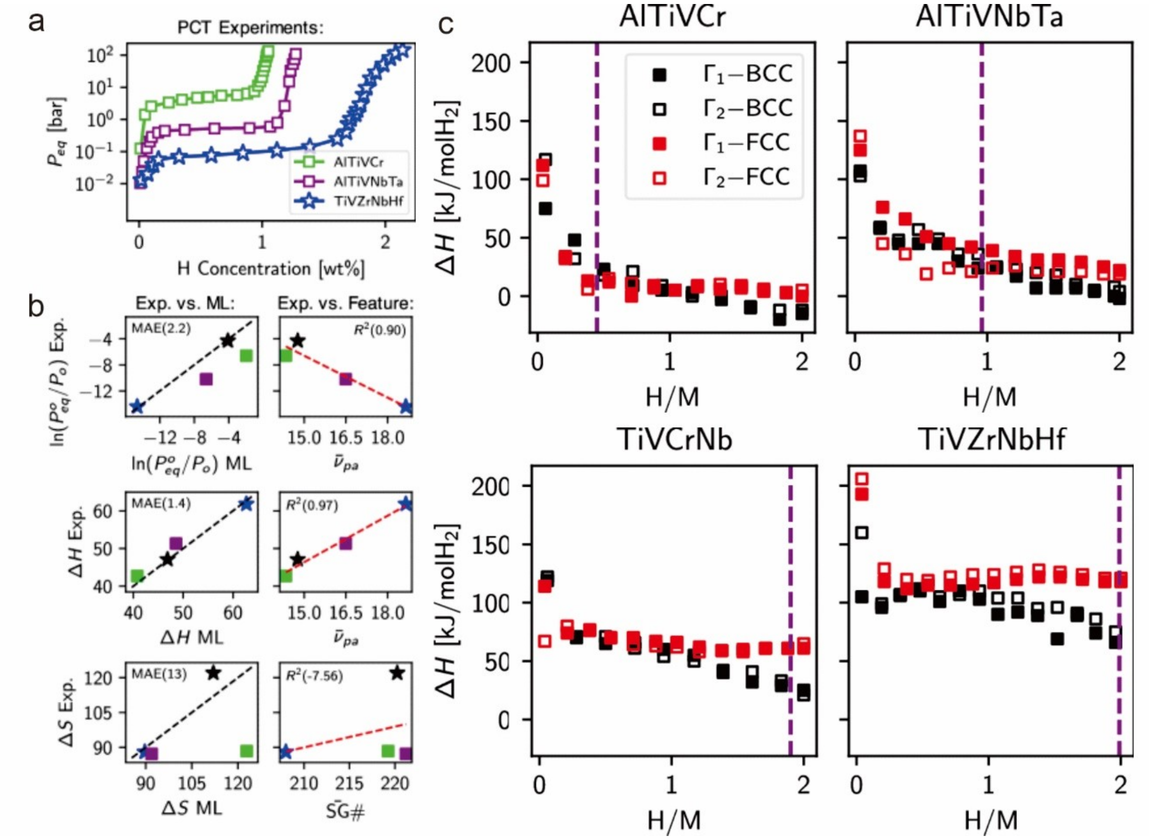

Figure 10. (a) Absorption PCT isotherms at 578, 561, and 571 K for TiVZrNbHf, AlTiVNbTa, and AlTiVCr, respectively. (b) Experimental hydriding thermodynamics vs ML predictions (left column) and the most important feature for each model (right column) with color-coding consistent with (a). (c) DFT-calculated hydride desorption enthalpy as a function of hydrogen loading (H/M ratio) for different HEA compositions in either the BCC or FCC lattice. Reproduced with permission from ref. 111 from the American Chemical Society, Copyright 2021.

Finally, to transition metal hydrides from laboratory scales to industrial applications, novel synthesis methods must be developed. For example, supercritical fluid deposition could emerge as a key technology, offering several benefits for the deposition of hydride materials onto support structures. This method significantly enhances their surface area and accessibility, and offers advantages in terms of material quality, process control, environmental impact, and applicability to advanced material systems. Additionally, several startups and companies are actively engaged in advancing metal hydride technology. Examples include GKN Automotive and Anspanner, showcasing the practical potential of metal hydrides in various applications. Various *in situ* techniques, such as electron microscopy and synchrotron radiation, can also provide direct insights into the behavior of metal hydrides under high pressure, offering valuable ideas for new material development.

3.3 Kubas interaction

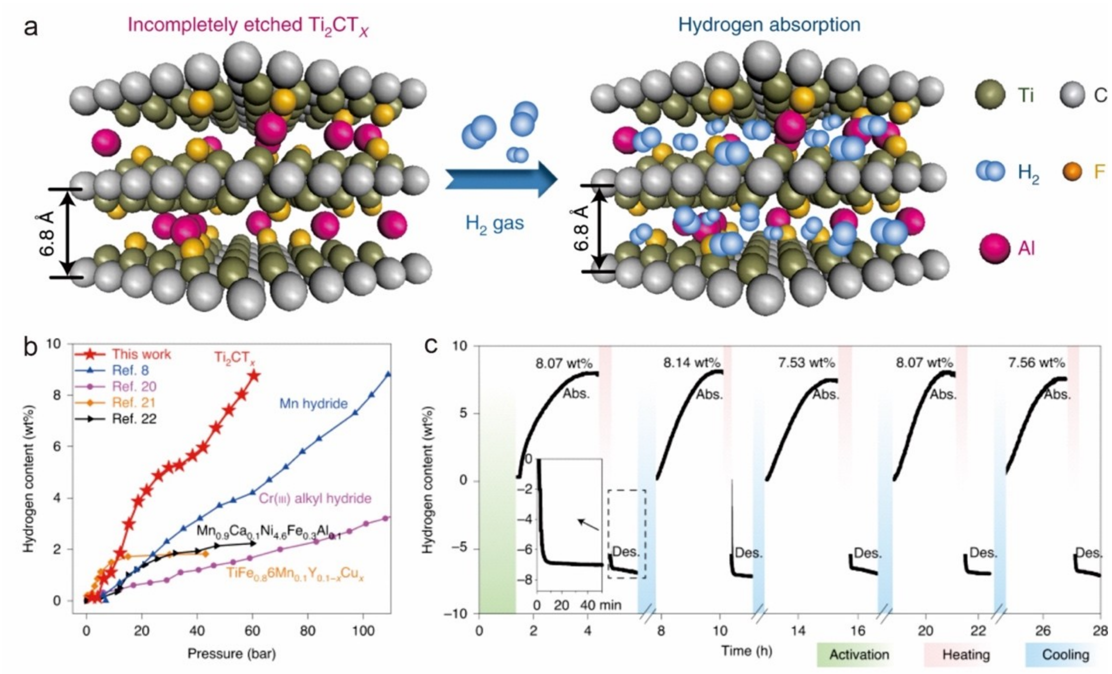

Figure 11. (a) Schematic of the H_2 storage process in the narrow interlayer space of Ti_2CT_x. (b) Comparison of H_2 isotherm curves of Ti_2CT_x with some representative room-temperature H_2 storage materials, namely, Kubas-type materials and metal hydride. (c) H_2 absorption and desorption curves of Ti_2CT_x in the initial several cycles. abs., absorption; Des., desorption. Inset: enlarged view of the desorption process. Reproduced with permission from ref. 115 from Nature publishing group, Copyright 2021.

The combination of the Kubas interaction with high surface area demonstrates significant potential to occupy a strong position in solid-state hydrogen storage. Recently, Shui et al. discussed the innovative application of a Kubas-type material, specifically the incompletely etched multilayer Ti_2CT_x, which achieves a remarkable H_2 uptake of 10.5 wt% under a pressure of 120 bar at room temperature (**Figure 11a-b**).[115] This material maintains its performance across multiple cycles, with minimal change in structural composition (**Figure 11c**). This consistency suggests that Ti_2CT_x could potentially meet the U.S. DOE targets for H_2 storage systems. Unlike traditional metal hydrides, the H_2 adsorption-desorption mechanism in this Kubas-type material exhibits a linear dependence on H_2 pressure, underscoring the necessity of maintaining high H_2 pressure for effective storage. This characteristic marks a significant departure from conventional H_2 storage methods that rely on strong chemical bonds or physical adsorption. Regarding the cycle in terms of pressure, it is important to clarify that while high pressure is necessary for effective H_{2i}adsorption, it may not be required for desorption. The desorption process may occur under lower pressure or even at ambient pressure, depending on the specific characteristics of the material and the conditions of the desorption process. In details, Ti_2CT_x is derived from the parent compound Ti_2AlC through an incomplete hydrofluoric acid etching process, resulting in a structure with a narrow interlayer distance favorable for H_2 storage. A notable feature of Ti_2CT_x is its capacity to retain about 4 wt% H_2 even under ambient conditions (25°C and 1 bar air), and its ability to uptake over 8.8 wt% H_2 under 60 bar pressure at room temperature, significantly surpassing previously reported materials under similar conditions. The authors attribute the storage mechanism of Ti_2CT_x to a nanopump-effect-assisted weak chemisorption within the sub-nanoscale interlayer space, facilitated by the presence of fluorine groups and the specific narrow interlayer distance maintained by residual Al atoms. The development of this Ti_2CT_x material for H_2 storage marks a significant step forward in realizing the practical application of H_2 as an energy vector. While the initial findings are promising, there are several perspectives to consider for advancing this technology towards commercialization and widespread adoption.

For example, the ability of Kubas-based materials to store H_2 at near-ambient conditions with minimal energy input aligns well with the goal of designing H_2 storage systems that are self-sustaining and require little other energy input. For example, H_2 is only released from the storage system and delivered to an end user when there are limited renewables to drive the electrolyzer generating low-carbon hydrogen. Without a battery, it is unlikely renewable electricity would be available to drive the release of H_2 from the storage system, and as such, any energy requirement for discharging H_2 will need to be served by the grid, fossil, or the H_2 itself. However, a major challenge lies in the limited number of materials that exhibit the Kubas interaction, typically restricted to those containing specific transition metals. In fact, the unique combination of accessible *d*-orbitals, variable oxidation states, and the ability to form stable complexes with H_2 makes specific transition metals ideal for facilitating Kubas interactions. This specificity is why the interaction is not commonly associated with other elements that lack these critical electronic and structural characteristics, which narrows the scope of materials available for development and poses a significant barrier to widespread application.

As a class of 2D materials with highly tunable surface functionalities, MXenes are characterized by their enriched element choice, unique surface chemical properties, and high surface area, making them ideal candidates for facilitating Kubas interactions as mentioned above. The surface functionalization of MXenes can be further optimized to enhance interactions with H_2, thereby increasing H_2 storage capacity and reaction kinetics. Leveraging the ability of MXenes to store H_2 through Kubas interactions at ambient conditions could lead to the development of energy efficient H_2 storage solutions. Unfortunately, MXenes are prone to oxidation in the environment, necessitating further modification to improve their stability and durability in practical applications. Additionally, the technology for mass production of high-quality MXenes is still immature, and production costs are relatively high. Moreover, due to the HF etching process used in their production, there is variability in the stability of MXenes produced by different groups. This inconsistency can lead to highly variable results in H_2 storage applications, even when the same materials are used. Therefore, for large-scale H_2 storage applications, reducing the production costs of MXenes with accurate control is a critical issue. We believe that in this field, researchers need to first develop new technologies to precisely control the growth and functionalization of MXenes, which can improve the uniformity and controllability of active sites on their surface, thereby enhancing their Kubas interaction capabilities with H_2. Especially, it is essential to ensure the reproducibility of MXenes; also, by combining cutting-edge surface and interface engineering techniques, such as doping with external transition metals and introducing non-metal elements, the electronic properties and surface activity of MXenes can be effectively regulated, enhancing their H_2 storage performance and stability by even combining physisorption, chemisorption and Kubas interaction. We also believe it is also crucial to effectively use multiscale modeling and computer simulations to optimize the structure and functionalization strategies of MXenes, predict and design more efficient Kubas-type H_2 storage materials. This approach can predict material performance before experiments, guide experimental design, and accelerate the development cycle of materials.

Meanwhile, the multi-component nature of HEAs results in complex lattice structures, which can create various localized chemical environments and crystal defects, such as vacancies and dislocations. These structural heterogeneities may provide diverse active sites, facilitating the adsorption of H_2 molecules. We believe that in HEAs, the presence of various transition metals can form a complex electronic environment. These environments can regulate the electron density distribution on the alloy surface, thereby improving the interaction between H_2 molecules and metals. This control of the electronic environment is essential for Kubas interactions, as it relies on the metal centers' ability to supply and receive electrons. Moreover, the synergistic effect of different elements in the alloy can enhance the binding energy with H_2, thereby enhancing the stability and reversibility of Kubas interactions. For example, an alloy comprising Fe, Ni, and Co could provide a robust framework for σ-bond formation because of their partially filled *d*-electrons, while adding elements like Ru, Rh, and Pd can enhance the capacity for π-back bonding due to its ability to provide *d*-electrons to the antibonding σ* orbitals of H_2, thereby improving the overall H_2 storage capacity and reversibility of the system. By carefully selecting and balancing these elements in a HEA system, researchers can tailor the electronic properties and structural characteristics of the alloy to maximize its effectiveness in H_2 storage. Furthermore, the high melting point and mechanical strength of HEAs ensure structural stability during H_2 adsorption and desorption processes. This stability is necessary for efficient H_2 storage systems, especially during repeated cycling. Therefore, we believe that HEAs, through their unique microstructures, tunable electronic properties, and synergistic effects, can also provide a diversified and optimized platform for enhancing and stabilizing Kubas interactions. Future research can further explore the impact of different HEA combinations on Kubas interactions, thereby achieving breakthroughs in the field of solid-state H_2 storage.

4. Market Potential and Commercialization Pathway

While nanomaterials have the potential to play a significant role in H_2 storage, just as they have in batteries, achieving this requires overcoming specific technical hurdles. Currently, solid-state H_2

storage is experiencing increasing engagement from various companies and research institutions, but such storage systems must demonstrate safety, land-, energy- and material-efficiency, limited loss of H_2 product, and functional coupling with H_2 supply and H_2 end use. These advancements are critical for widespread adoption, particularly in small to medium size applications of H_2. As bulk storage (100s to 1000s of tonnes) of H_2 is necessary for industry and large-scale renewable generation storage, we do not see these applications as near term for solid-state storage. The sheer magnitude of solid storage material, and the inherent safety and maintenance issues related to managing thousands of storage tanks and associated piping and balance of plant is likely to be impractical. Other storage solutions like underground storage in salt caverns, or potential liquid organic hydrogen carriers may perform more practically in such large applications. [116] We note that while the focus of this section is on technical and economic performance, there is a glaring research gap associated with the carbon intensity of storage systems, and with the sustainability of material manufacturing and material end of life.

Nanomaterials-based H_2 storage systems have been successfully demonstrated in the laboratories and on prototype vehicles.[117] Notably, Bevan et al. demonstrated a 4 kg H_2 storage capability using $TiMn_2$-based metal hydride in a canal boat, achieving a desorption flow rate and temperature suitable for operating a 1 kW proton exchange membrane fuel cell in a water-based environment.[118] In the realm of energy storage and power-to-power energy applications, H2GO Power offers a long-duration H_2 storage module, enabling efficient H_2 delivery for high-power applications. GKN Hydrogen employs metal hydride for H_2 storage in various applications including backup systems, microgrids, and seasonal storage. Their product lineup—HY2MINI, HY2MEDI, and HY2MEGA—demonstrates scalability from small to large storage needs. These examples highlight the growing application of solid-state H_2 storage technologies across a range of energy sectors.

Numerous theoretical and experimental studies have emerged to not only characterize but set targets for the material properties and general trends in how materials should behave for solid-state H_2 storage.[3, 12, 55, 119] TEA for solid-state H_2 storage is crucial for evaluating both the technical performance and economic viability of these systems. By assessing factors such as system energy efficiency, system costs including levelized cost of storage (LCOS) ($/kWh), and levelized cost of energy (LCOE),[120] and life-cycle impacts related to material manufacturing and energy provision, researchers can identify the most promising materials that balance performance with cost-effectiveness. This analysis is vital for assessing the competitiveness of solid-state H_2 storage against other methods like compressed gas and liquid H_2, as well as incumbent and emerging energy storage technologies such as batteries.[121] However, translating these insights into material-level information that can help scientists guide future research and development is a challenge, as TEA models often miss the granularity and modeling sophistication to capture the impact of material tuning beyond high-level energy balance, volumetric (kWh/L) and gravimetric density (kWh/kg) effects.

As such, TEA have emerged that are experiment informed and employ a variety of analytical methods to represent and guide reactor design, kinetics, thermal management and process intensification. Key factors to consider even before a process model is constructed in software such as ASPENPlus or mathematically include system definition[122]: clarifying whether the H_2 storage is intended for transportation or stationary energy storage, geographic location, year of deployment, the deployment scale of such systems to inform material manufacturing scales, the overall operation cycle per year and per system lifetime, what the final product is and at what rate and quality (e.g. electricity, H_2, byproducts). If a model material and model storage system is not available to represent the reaction performance and kinetics, the TEA must start with a thorough materials analysis to identify representative materials with adequate characterization data to simplify the generalization of the model to other materials in the same class. Thankfully such models have now emerged for a wide range of sorbent materials and now metal hydrides, some of which are discussed in the following sections.

To effectively model cost and energy flows for different H_2 storage materials, robust and accurate experimental data are essential.[122] At a minimum, a material characterization dataset should include: (1) Information to approximate uptake at specific conditions relevant to practical storage. For hydrides this will include H_2 pressure-composition-temperature (PCT) curves, crucial for understanding H_2 capacity under various conditions including the temperature and pressure at which H_2 is released. For sorbents this will include isotherms. (2) Heat enthalpy of charging and discharging, which indicates the energy requirements during H_2 uptake and release, and sensitivities of the material to exceeding certain temperatures, potentially necessitating costlier thermal management. (3) Thermal properties such as thermal conductivity, heat capacity and composition including doping and filler components for pellet which affects tank material selection, design, and specifying the corresponding equipment such as heat exchangers, refrigeration units, compressors, and heaters. (4) Measurements or approximations of physical properties including skeletal density, porosity, and packing efficiency. (5) Kinetics of hydrogenation and dehydrogenation which are linked to the application system definition and will have major implications for the capacity sizing of the balance of plant (MW size of refrigeration for example) and thus capital costs. (6) Material cyclability, durability and feasible depth of discharge impacting overall storage capacity, first fill material requirement, and replacement. (7) Material sensitivity to impurities and material cost. Additionally, operating conditions, including the necessary temperature and pressure conditions for efficient H_2 charging and discharging, must be identified, and care should be taken when considering projections of H_2 uptake and kinetics at conditions outside of published experimental measurements. Other key factors that greatly affect overall costs such as safety regulations and labor must be approximated from expert input and chemical engineering rules of thumb.

4.1 TEA for transportation applications

Transportation applications on road, rail, air, and sea impose stringent requirements on system weight, space, and dynamic operations.[123] The U.S. DOE has set the 2025 technical targets for onboard H_2 storage for light-duty vehicles (LDVs), aiming for a gravimetric energy density 1.8 kWh/kg and volumetric energy density 1.3 kWh/L by 2025.[124] To facilitate the development of solid-state material hydrogen storage systems, tools such as the "Design tool" and "Tankinator models" have been developed.[125, 126] These tools allow users to estimate the H_2 storage tank size and energy density based on the input material properties for H_2 fuel cell LDVs.[125, 126]. A comprehensive analysis of sorbents for use in automotive hydrogen storage systems has been conducted.[123] The findings indicate that to meet performance benchmarks -5.5 wt% gravimetric capacity, 44 g/L volumetric capacity, 55% well-to-tank efficiency, 95% usable H2 and a refueling rate of 1.5 kg/min – the following minimum physical and thermodynamics requirements must be met: The promising sorbent should achieve an excess hydrogen capacity of 120 g/kg at a temperature of 150 K or above and a pressure of 100 bar. Additionally, it should exhibit a differential enthalpy of adsorption of 5 kJ/mol and a thermal conductivity of 1 W/m/K when combined with up to 20 wt% expanded natural graphite. The bulk density of the mixture should be compacted to 420 kg/m^3. TEA for bulk H_2 transportation suggests that the levelized cost of long-distance transmission using MOF-based truck fleets ranges from \$7.3 to \$29 per kg of H_2, which is more expensive than the \$1.8/kg for 350 bar compressed gas.[127] One of the major challenges identified in this application for sorbents is the necessary precooling of both the H_2 coming hot off the electrolyzer, and the onboard tanks themselves.

Metal hydrides offer good volumetric energy density but fall short in gravimetric energy density due to the mass of heavy metals and the complexity of thermal management systems, making their usage in passenger vehicles impractical.[128] Although most complex metal hydrides meet the energy density requirement, their slow kinetics and high operating temperatures make them unsuitable for passenger cars or truck fleets which require fast fills.[129] A cost analysis of the $NaAlH_4$ storage system for onboard applications shows that to store 5.6 kg of H_2, the system attains a gravimetric energy density of 0.0122 kg/kg and a volumetric energy density of 0.0115 kg/L, both metrics significantly short of the targets set by DOE.[130] In addition, the estimated cost of that system is \$42.9 per kWh, substantially exceeding the DOE's 2025 target of \$9 per kWh. This high cost is primarily attributed to the expenses associated with the dual tanks and related components. The cost of the metal hydride for $Mg(NH_2)_2$-LiH storing 4 kg of H_2 is estimated to be between \$28,000 and \$35,000. Factoring in higher initial costs, for production of 1,000 units, the cost of the tank could be reduced to approximately \$8,075 to \$10,100.[131] For rail applications, high-capacity hydrides such as $TiFeH_2$ are heavy, causing gross weight to exceed the maximum allowable on U.S. track. Consequently, the most attractive hydrides are those with the highest gravimetric capacities: MgH_2 and lithium-magnesium amide.[132] However, these materials face challenges due to their high operating temperatures and slow kinetics.[133] For aerospace applications, sodium borohydride has been explored for unmanned aerial vehicles (UAVs).[134] When integrated with a PEM fuel cell, this system can deliver a 900 Wh of energy from 1 liter of chemical solution. However, managing the temperature within the hydride system presents significant challenges. Further research should focus on enhancing the reactivity and thermal management to enhance the overall system's performance and reliability. The additional weight of the metal hydrides materials suits submarines, which require extra weight to balance the buoyancy. German and Italian Navy already employ metal hydride based submarines (Class U212A and 214).[135] Another study shows that 120 g/dm^3 for the volumetric capacity and 150 charge and discharge cycles can be achieved for hydrides in submarine applications.[136] TEA analysis for refueling a small H_2-powered vessel indicates that the simpler refueling needs of metal hydride-based onboard tanks result in a significant cost reduction of the H_2 handling equipment, with investment costs of metal hydride-based storage ranging from 3400 to 7300 EUR/kg H_2, competitive with compressed gas H_2 storage.[137] Among the MH storage systems examined, the current materials and refueling concepts are not suitable for road and commercial aviation applications due to their high weight and slow refueling rates.[134, 138] While weight is less critical for ship applications, future R&D efforts should focus on enhancing the charging and discharging rates of MHs and optimizing thermal management, or find methods for charging solid-state storage tanks prior to loading onto transportation vessels

4.2 TEA for stationary energy storage applications

Solid-state H_2 storage can also be applied in stationary power applications. Due to the seasonality of renewable energy sources like wind and solar power, seasonal and long-duration energy storage is an attractive solution, where renewable energy is converted to H_2 for storage and then back to electricity using fuel cells. Unlike vehicular applications, where space and mass are limited and where gravimetric and volumetric energy densities are critical factors, stationary long-duration H_2 storage applications are evaluated based on reliability, H_2 purity, charge temperature and pressure, charge and discharge rates, scalability, and cost.[129] For example, the Breunig group provides an in-depth analysis of MOFs for H_2 storage, specifically targeting their application in bulk transportation[127] and in stationary back-up power systems, as summarized in **Figure 12**,[122] , in which they find that when the MOFs are packed loosely (under bed and pellet porosities of 0.6), all of the modelled MOFs are more economical than liquid H_2 storage and have the potential of being economically comparable with compressed gas storage. The work also emphasizes the role of H_2 as an efficient and sustainable energy storage solution, particularly beneficial for maintaining uninterrupted power supply in energy-intensive infrastructures such as data centers and hospitals. The study underscores the environmental and operational drawbacks of traditional fossil-fuel generators and positions H_2, in combination with MOFs, as a viable alternative that could potentially exceed the performance and economic viability of current systems, especially for power support durations beyond 10 hours. It also identifies key performance benchmarks that MOFs need to achieve to be economically competitive, including a H_2 adsorption capacity of at least 15 g/kg and a production cost reduction to below \$10/kg. These targets highlight the necessary advancements in material science required to make MOFs a practical option for back-up power applications. Furthermore, the study discusses the unique properties of MOFs, such as high surface areas and the capability of undergoing a phase change upon H_2 loading, which could enhance the storage capacity and prevent H_2 loss during low-pressure cycles. However, it points out challenges such as poor heat transport within MOFs, which could impact the efficiency of the system at scale.

It has been suggested that emerging MOFs using abundant metals like Ni or Zn could achieve a material cost of \$10/kg of MOF.[139] In which, production costs for four MOFs have been reported, with baseline costs ranging from \$35/kg to \$71/kg. With manufacturing optimizations and reductions in the costs of linkers and metal precursors, these expenses could potentially be reduced to below \$10/kg. Using an aqueous solution-based method, the production cost of UiO-66-NH_2 was estimated at \$15.8/kg.[140] Reducing the manufacturing cost of ALF to approximately \$2/kg is achievable, given that it utilizes widely available commodity chemicals aluminum hydroxide and formic acid and avoids the use of comparatively complex organic reagents.[61] Lowering the manufacturing price of these materials could significantly reduce the capital cost of storage materials, thereby making them competitive with other system components such as refrigeration units and compressors. Given these results, commercializing MOF seems feasible; however, the scalability of production costs remains a crucial factor, especially for stationary energy storage applications that may require large quantities of material to store substantial amounts of H_2. Additionally, the operating cost for energy usage during the charging and discharging process is also a critical consideration. MOF systems can achieve higher H_2 uptake at high pressure and low temperature, but it is crucial to determine whether the benefits of higher uptake outweigh the energy costs of operating under these conditions. Depending on the material properties and specific applications, the optimal operating conditions may vary.

Compared to traditional physical based methods, metal hydrides can also store appreciable amounts of H_2 at moderate to low pressures, suitable for stationary H_2 storage.[141] Low-pressure operation is compelling, as a storage pressure between 10 and 30 bar is sufficient to meet the pressure requirements of stationary fuel cells operating at 2 to 5 bar,[142] and without the need for compressor, as the typical pressure of H_2 gas from electrolyzer is 30 bar.[143] Beyond economic considerations, operating storage systems at low pressures greatly reduces the safety concerns and system complexity.[144] Since no H_2 is lost during storage, metal hydrides are ideal for mid-to-long term H_2 storage for applications such as backup power, seasonal storage, and off-grid system. Recent progress in their development for serving stationary long duration energy storage applications has been benchmarked against system-level performance targets ranging from cost to land footprint within HyMARC, with modeling tools to be released soon. The main capital cost for metal hydrides based stationary H_2 storage is attributed to the price of metal hydrides. Hence, materials like Ti, Zr or Mg, which are relatively low-priced, are preferred. Mg, in particular, has been commercialized in powder and pellets at prices ranging from \$2.30 to

$823/kg, depending on the required particle size. Operating costs include heating and cooling during the dehydriding and hydrating process, respectively. The amount of heat required depend on the heat enthalpy of materials and specific applications. For example, if metal hydride system is integrated with fuel cells or an industry power plant, the heating demand might be met by the waste heat from the cooling load of these applications. Low-temperature metal hydrides would integrate well with proton exchange membrane fuel cells operating at 353 K, thereby reducing operation costs.

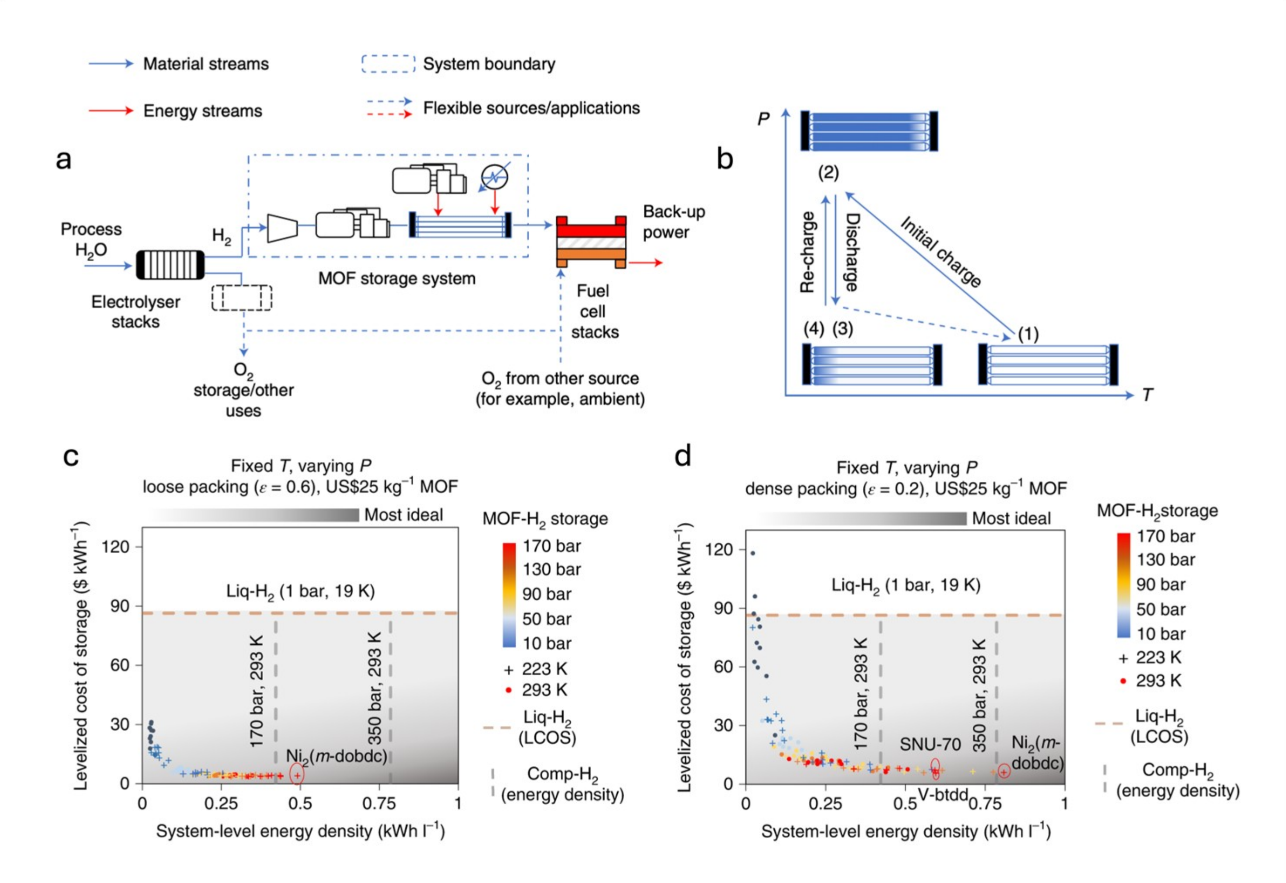

Figure 12. Process flow and system performance utilizing MOF for hydrogen storage in the back-up power system. (a) System boundary and main unit equipment for hydrogen storage using MOF. (b) Overview of the temperature and pressure conditions across different operational stages. (c)-(d) Performance of promising MOF under loose packing conditions and dense packing conditions against traditional physical hydrogen storage methods respectively. Reproduced with permission from ref. 122 from Nature publishing group, Copyright 2022.

4.3 Current challenges and future directions in TEA for solid-state material H_2 storage

While solid-state H_2 storage offers promising tunability and opens a broad spectrum for material discovery, we are currently still at the development stage of requiring costly laboratory tests and computational simulations to improve measurement of H_2 capacity and assess material physical and thermal properties. From here, we must rapidly move into demonstrations and pilots that can validate performance and provide unique insights into thermal management and system operation that analytical methods can only approximate. ML emerges as a promising solution to address these computationally complex challenges, but there must be suitable data to train on. It has been effectively used to predict H_2 uptake and thermal properties in MOFs and metal hydrides, thereby guiding new material design and development.[111, 145-151] However, most current ML predictions for H_2 uptake in MOFs are limited to 77K, and there is a lack of data on accurately predicting metal hydrides PCT curves. The ability to predict H_2 capacity across various pressures and temperatures is highly desirable as it facilitates screening of candidate materials for critical applications where we know much about real-world operating conditions.

Accurate measurements of H_2 uptake in solid-state materials and the determination of PCT curves are important for assessing H_2 capacity and heat of enthalpy. The primary measurement techniques currently employed include volumetric measurements, gravimetric measurements, and temperature-programmed desorption (TPD), each with its inherent limitations.[152] For instance, volumetric measurements can suffer from errors dur to poorly calibrated internal volumes and inaccurate pressure measurements. Leaks and poor temperature control can largely affect the accuracy of measurements. In gravimetric measurements, errors may originate from instability of the microbalance and from the sorption of impurities that will result in a larger weight signal per mole than H_2 itself. For the TPD method is susceptible to errors from by inaccurate calibration. In addition, a fundamental concern is the consistency between lab-scale material production and measurement versus industrial-scale processes. It has been observed that the $TiFe_{0.85}Mn_{0.05}$ alloy has different microstructure, phase abundance and surfaces properties when prepared at industrial level by induction melting, compared to the same composition prepared at laboratory scale.[153] These variations, induced by differences in the synthesis process, significantly impact the activation process, absorption capacities and reaction kinetics.

Moreover, advancements in materials and manufacturing processes are significant drivers for cost reduction and market growth. To date, however, the majority of research efforts on material-based H_2 storage have focused on developing new materials with improved H_2 uptakes, with limited data available on solid-state material costs.[61, 139] Manufacturing analyses can predict likely processes at certain manufacturing scales based on industrial analogues, consultations with specialized manufacturers, and lab-scale synthesis techniques. Although over 14,000 different MOFs have been documented with their material-based properties in the CORE database—a number that continues to grow—data on their production costs and environmental impact at scale are very limited.[154] While an increase in H_2 uptake performance and durability is important and can reduce the material quantity required within the system, if this increase comes at the cost of very expensive raw materials or complex manufacturing processes, it will not outcompete compressed gas storage. Additionally, as material costs are significant cost contributors, we believe that developing the recycling of solid-state materials should be a focus for future research.

Additionally, the kinetic performance for metal hydrides based H_2 storage is critical, particularly for transportation applications. H_2 absorption in metal hydrides involves a multi-phase reaction, with different energy barriers at each stage that must be considered. Strategies to improve kinetics include but are not limited to nano-crystallization and the addition of catalysis.[155] It is important to incorporate detailed kinetics data for various metal hydrides into future TEA to better understand the feasibility and applicability of their applications.

Finally, in addition to material uptake and cost, the cyclability and degradation of materials such as MOFs and metal hydrides are crucial for their competitiveness in H_2 storage applications. For stationary energy storage, only 8-30 cycles per year may be required, but applications like peak shaving and vehicle operations might need daily or weekly cycles. For instance, the U.S. DOE has established technical targets for onboard H_2 storage in LDVs, requiring a lifecycle of 1500 operational cycles. Materials that demonstrate long cycle stability will not only reduce the costs of raw materials but also minimize associated replacement expenses. However, the existing literature on the cyclability of metal hydrides is limited. Developing standardized testing protocols to evaluate cyclability under realistic operational conditions will facilitate effective benchmarking of different solid-state materials and technologies.

5. Conclusion

In summary, we believe that solid-state H_2 storage based on nano-sized materials offers an innovative approach to overcoming the challenges associated with traditional high-pressure and cryogenic storage methods utilized in H_2 technologies. By integrating advanced materials such as MOFs, Mg-based hybrids, and novel sorbents, this field has seen significant advancements. This work encapsulates the current state of technology and sets forth a vision for future developments, emphasizing the necessity for continued innovation in material science to achieve higher storage capacities and cost-effectiveness. Future research directions may include exploring HEAs and further developing MXenes to enhance the performance and application range of hydrogen storage systems. System-level integration, alongside the development of computational modeling and high-throughput screening, is crucial for better identifying the materials or material properties that best match target end uses to help focus research and industry investment. These advancements could help transition H_2 storage from a research concept to a practical component of global energy systems, playing a critical role in the transition towards renewable energy systems by enabling a more reliable and flexible energy infrastructure. System-level insights guide the development and implementation of solid-state H_2 storage technologies, only when the approaches used have the sophistication to simulate the effects of material-level innovations on overall performance. From there, engineering design and analysis can inform whether the pursuit of ambient condition operation or other such challenging experimental targets, are actually necessary for outcompeting conventional storage. Breakthroughs are necessary, and preliminary TEA suggests solid-state storage has only just begun to break even with 350 bar compressed gas storage systems. With advancements in material synthesis, characterization, and coupling with computational approaches, even greater progress can be made in the coming decade. Ongoing challenges such as the identification of cost-reducing and energy saving operation conditions specific to end uses and materials, the scalability of production methods, and the enhancement of storage capacities and kinetics through advanced material engineering remain critical hurdles. Addressing these challenges through innovative manufacturing processes like supercritical fluid deposition, is essential for advancing the practical application of H_2 storage technologies and fully realizing the potential of H_2 as a cornerstone of sustainable energy systems.

Acknowledgement

Work at the Molecular Foundry were supported by the Office of Science, Office of Basic Energy Sciences, of the U.S. Department of Energy under Contract No. DE-AC02-05CH11231. The authors gratefully acknowledge funding provided by U.S. Department of Energy Office of Energy Efficiency and Renewable Energy Hydrogen and Fuel Cell Technologies Office. This work was also performed in part under the auspices of DOE by Lawrence Livermore National Laboratory under Contract DE-AC52-07NA27344. The United States Government retains, and the publisher, by accepting the article for publication, acknowledges that the United States Government retains a nonexclusive, paid-up, irrevocable, worldwide license to publish or reproduce the published form of this manuscript, or allow others to do so, for United States Government purposes.

References

[1] He, T.;Pachfule, P.;Wu, H.;Xu, Q.; Chen, P. Hydrogen carriers. *Nat Rev Mater* **2016**, *1*.

[2] Li, G. Q.;Kobayashi, H.;Taylor, J. M.;Ikeda, R.;Kubota, Y.;Kato, K.;Takata, M.;Yamamoto, T.;Toh, S.;Matsumura, S.; Kitagawa, H. Hydrogen storage in Pd nanocrystals covered with a metal-organic framework. *Nat Mater* **2014**, *13*, 802-806.

[3] Chen, Z. J.;Kirlikovali, K. O.;Idrees, K. B.;Wasson, M. C.; Farha, O. K. Porous materials for hydrogen storage. *Chem-Us* **2022**, *8*, 693-716.

[4] Nasser, M.; Hassan, H. Techno-enviro-economic analysis of hydrogen production via low and high temperature electrolyzers powered by PV/Wind turbines/Waste heat. *Energ Convers Manage* **2023**, *278*.

[5] Boretti, A. Electric vehicles with small batteries and high-efficiency on-board electricity production. *Energy Storage* **2019**, *1*.

[6] Sikiru, S.;Oladosu, T. L.;Amosa, T. I.;Olutoki, J. O.;Ansari, M. N. M.;Abioye, K. J.;Rehman, Z. U.; Soleimani, H. Hydrogen-powered horizons: Transformative technologies in clean energy generation, distribution, and storage for sustainable innovation. *Int J Hydrogen Energ* **2024**, *56*, 1152-1182.

[7] Yue, M. L.;Lambert, H.;Pahon, E.;Roche, R.;Jemei, S.; Hissel, D. Hydrogen energy systems: A critical review of technologies, applications, trends and challenges. *Renew Sust Energ Rev* **2021**, *146*.

[8] Ball, M.; Weeda, M. The hydrogen economy - Vision or reality? *Int J Hydrogen Energ* **2015**, *40*, 7903-7919.

[9] Olabi, A. G.;Bahri, A. S.;Abdelghafar, A. A.;Baroutaji, A.;Sayed, E. T.;Alami, A. H.;Rezk, H.; Abdelkareem, M. A. Large-vscale hydrogen production and storage technologies: Current status and future directions. *Int J Hydrogen Energ* **2021**, *46*, 23498-23528.

[10] Nadeem, F.;Hussain, S. M. S.;Tiwari, P. K.;Goswami, A. K.; Ustun, T. S. Comparative Review of Energy Storage Systems, Their Roles, and Impacts on Future Power Systems. *Ieee Access* **2019**, *7*, 4555-4585.

[11] Lehmann, M. L.;Tyler, L.;Self, E. C.;Yang, G.;Nanda, J.; Saito, T. Membrane design for non-aqueous redox flow batteries: Current status and path forward. *Chem-Us* **2022**, *8*, 1611-1636.

[12] García-Holley, P.;Schweitzer, B.;Islamoglu, T.;Liu, Y. Y.;Lin, L.;Rodriguez, S.;Weston, M. H.;Hupp, J. T.;Gómez-Gualdrón, D. A.;Yildirim, T.; Farha, O. K. Benchmark Study of Hydrogen Storage in Metal-Organic Frameworks under Temperature and Pressure Swing Conditions. *Acs Energy Lett* **2018**, *3*, 748-754.

[13] Zheng, J. Y.;Liu, X. X.;Xu, P.;Liu, P. F.;Zhao, Y. Z.; Yang, J. Development of high pressure gaseous hydrogen storage technologies. *Int J Hydrogen Energ* **2012**, *37*, 1048-1057.

[14] Monteiro, E.; Brito, P. S. D. Hydrogen supply chain: Current status and prospects. *Energy Storage* **2023**, *5*.

[15] Ratnakar, R. R.;Gupta, N.;Zhang, K.;van Doorne, C.;Fesmire, J.;Dindoruk, B.; Balakotaiah, V. Hydrogen supply chain and challenges in large-scale LH2 storage and transportation. *Int J Hydrogen Energ* **2021**, *46*, 24149-24168.

[16] Reznicek, E. P. a. K., Mariya and King, Jennifer and Kotarbinski, Matthew and Grant, Elenya Sophia and Vijayshankar, Sanjana and Brunik, Kaitlin and Thomas, Jared and Gupta, Abhineet and Hammond, Steven and Singh, Vivek and Tusing, Richard and Sun, Pingping and Lee, Kyuha and Elgowainy, Amgad and Breunig, Hanna and Rosner, Fabian and Pinto, João Pereira, Techno-Economic Analysis of Low-Carbon Hydrogen Production Pathways for Decarbonizing Steel and Ammonia Production. *Joule* **2024**, http://dx.doi.org/10.2139/ssrn.4785779.

[17] Ramirez-Vidal, P.;Sdanghi, G.;Celzard, A.; Fierro, V. High hydrogen release by cryo-adsorption and compression on porous materials. *Int J Hydrogen Energ* **2022**, *47*, 8892-8915.

[18] Chen, M.;Wang, Y. Q.;Xiao, X. Z.;Lu, Y. H.;Zhang, M.;Zheng, J. G.; Chen, L. X. Highly efficient ZrH nanocatalyst for the superior hydrogenation kinetics of magnesium hydride

under moderate conditions: Investigation and mechanistic insights. *Appl Surf Sci* **2021**, *541*.

[19] Majumdar, A.;Deutch, J. M.;Prasher, R. S.; Griffin, T. P. A framework for a hydrogen economy Comment. *Joule* **2021**, *5*, 1905-1908.

[20] Allendorf, M. D.;Hulvey, Z.;Gennett, T.;Ahmed, A.;Autrey, T.;Camp, J.;Cho, E. S.;Furukawa, H.;Haranczyk, M.;Head-Gordon, M.;Jeong, S.;Karkamkar, A.;Liu, D. J.;Long, J. R.;Meihaus, K. R.;Nayyar, I. H.;Nazarov, R.;Siegel, D. J.;Stavila, V.;Urban, J. J.;Veccham, S. P.; Wood, B. C. An assessment of strategies for the development of solid-state adsorbents for vehicular hydrogen storage. *Energ Environ Sci* **2018**, *11*, 2784-2812.

[21] Santhosh, A.;Kang, S. Y.;Keilbart, N.;Wood, B. C.;Klassen, T.;Jerabek, P.; Dornheim, M. Influence of near-surface oxide layers on TiFe hydrogenation: mechanistic insights and implications for hydrogen storage applications. *J Mater Chem A* **2023**, *11*, 18776-18789.

[22] Ding, F.; Yakobson, B. I. Challenges in hydrogen adsorptions: from physisorption to chemisorption. *Front Phys-Beijing* **2011**, *6*, 142-150.

[23] Niaz, S.;Manzoor, T.; Pandith, A. H. Hydrogen storage: Materials, methods and perspectives. *Renew Sust Energ Rev* **2015**, *50*, 457-469.

[24] Thommes, M.;Kaneko, K.;Neimark, A. V.;Olivier, J. P.;Rodriguez-Reinoso, F.;Rouquerol, J.; Sing, K. S. W. Physisorption of gases, with special reference to the evaluation of surface area and pore size distribution (IUPAC Technical Report). *Pure Appl Chem* **2015**, *87*, 1051-1069.

[25] Zuttel, A.;Sudan, P.;Mauron, P.;Kiyobayashi, T.;Emmenegger, C.; Schlapbach, L. Hydrogen storage in carbon nanostructures. *Int J Hydrogen Energ* **2002**, *27*, 203-212.

[26] Zhou, Y. G.;Zu, X. T.;Gao, F.;Nie, J. L.; Xiao, H. Y. Adsorption of hydrogen on boron-doped graphene: A first-principles prediction. *J Appl Phys* **2009**, *105*.

[27] Ataca, C.;Akturk, E.;Ciraci, S.; Ustunel, H. High-capacity hydrogen storage by metallized graphene. *Appl Phys Lett* **2008**, *93*.

[28] Tozzini, V.; Pellegrini, V. Prospects for hydrogen storage in graphene. *Phys Chem Chem Phys* **2013**, *15*, 80-89.

[29] Patchkovskii, S.;Tse, J. S.;Yurchenko, S. N.;Zhechkov, L.;Heine, T.; Seifert, G. Graphene nanostructures as tunable storage media for molecular hydrogen. *P Natl Acad Sci USA* **2005**, *102*, 10439-10444.

[30] Barghi, S. H.;Tsotsis, T. T.; Sahimi, M. Chemisorption, physisorption and hysteresis during hydrogen storage in carbon nanotubes. *Int J Hydrogen Energ* **2014**, *39*, 1390-1397.

[31] Rather, S. U. Preparation, characterization and hydrogen storage studies of carbon nanotubes and their composites: A review. *Int J Hydrogen Energ* **2020**, *45*, 4653-4672.

[32] Mohan, M.;Sharma, V. K.;Kumar, E. A.; Gayathri, V. Hydrogen storage in carbon materials-A review. *Energy Storage* **2019**, *1*.

[33] Lyu, J. Z.;Kudiiarov, V.; Lider, A. An Overview of the Recent Progress in Modifications of Carbon Nanotubes for Hydrogen Adsorption. *Nanomaterials-Basel* **2020**, *10*.

[34] Mauron, P.;Remhof, A.;Bliersbach, A.;Borgschulte, A.;Zuttel, A.;Sheptyakov, D.;Gaboardi, M.;Choucair, M.;Pontiroli, D.;Aramini, M.;Gorreri, A.; Ricco, M. Reversible hydrogen absorption in sodium intercalated fullerenes. *Int J Hydrogen Energ* **2012**, *37*, 14307-14314.

[35] Langmi, H. W.;Ren, J. W.;North, B.;Mathe, M.; Bessarabov, D. Hydrogen Storage in Metal-Organic Frameworks: A Review. *Electrochim Acta* **2014**, *128*, 368-392.

[36] Furukawa, H.;Cordova, K. E.;O'Keeffe, M.; Yaghi, O. M. The Chemistry and Applications of Metal-Organic Frameworks. *Science* **2013**, *341*, 974-+.

[37] Li, H.;Wang, K. C.;Sun, Y. J.;Lollar, C. T.;Li, J. L.; Zhou, H. C. Recent advances in gas storage and separation using metal-organic frameworks. *Mater Today* **2018**, *21*, 108-121.

[38] Schoedel, A.;Ji, Z.; Yaghi, O. M. The role of metal-organic frameworks in a carbon-neutral energy cycle. *Nat Energy* **2016**, *1*.

[39] Rowsell, J. L. C.; Yaghi, O. M. Strategies for hydrogen storage in metal-organic frameworks. *Angew Chem Int Edit* **2005**, *44*, 4670-4679.

[40] Chen, M. H.;Li, H. R.;Liu, C. X.;Liu, J. Y.;Feng, Y. Q.;Wee, A. G. H.; Zhang, B. Porphyrin- and porphyrinoid-based covalent organic frameworks (COFs): From design, synthesis to applications. *Coordin Chem Rev* **2021**, *435*.

[41] Ding, S. Y.; Wang, W. Covalent organic frameworks (COFs): from design to applications. *Chem Soc Rev* **2013**, *42*, 548-568.

[42] Han, S. S.;Furukawa, H.;Yaghi, O. M.; Goddard, W. A. Covalent organic frameworks as exceptional hydrogen storage materials. *J Am Chem Soc* **2008**, *130*, 11580-+.

[43] Geng, K. Y.;He, T.;Liu, R. Y.;Dalapati, S.;Tan, K. T.;Li, Z. P.;Tao, S. S.;Gong, Y. F.;Jiang, Q. H.; Jiang, D. L. Covalent Organic Frameworks: Design, Synthesis, and Functions. *Chem Rev* **2020**, *120*, 8814-8933.

[44] Dong, J. X.;Wang, X. Y.;Xu, H.;Zhao, Q.; Li, J. P. Hydrogen storage in several microporous zeolites. *Int J Hydrogen Energ* **2007**, *32*, 4998-5004.

[45] Li, Y. W.; Yang, R. T. Hydrogen storage in low silica type X zeolites. *J Phys Chem B* **2006**, *110*, 17175-17181.

[46] Muthu, R. N.;Rajashabala, S.; Kannan, R. Hydrogen storage performance of lithium borohydride decorated activated hexagonal boron nitride nanocomposite for fuel cell applications. *Int J Hydrogen Energ* **2017**, *42*, 15586-15596.

[47] Rai, D. P.;Chettri, B.;Patra, P. K.; Sattar, S. Hydrogen Storage in Bilayer Hexagonal Boron Nitride: A First-Principles Study. *Acs Omega* **2021**, *6*, 30362-30370.

[48] Revabhai, P. M.;Singhal, R. K.;Basu, H.; Kailasa, S. K. Progress on boron nitride nanostructure materials: properties, synthesis and applications in hydrogen storage and analytical chemistry. *J Nanostructure Chem* **2023**, *13*, 1-41.

[49] Murray, L. J.;Dinca, M.; Long, J. R. Hydrogen storage in metal-organic frameworks. *Chem Soc Rev* **2009**, *38*, 1294-1314.

[50] Madden, D. G.;O'Nolan, D.;Rampal, N.;Babu, R.;Camur, C.;Al Shakhs, A. N.;Zhang, S. Y.;Rance, G. A.;Perez, J.;Casati, N. P. M.;Cuadrado-Collados, C.;O'Sullivan, D.;Rice, N. P.;Gennett, T.;Parilla, P.;Shulda, S.;Hurst, K. E.;Stavila, V.;Allendorf, M. D.;Silvestre-Albero, J.;Forse, A. C.;Champness, N. R.;Chapman, K. W.; Fairen-Jimenez, D. Densified HKUST-1 Monoliths as a Route to High Volumetric and Gravimetric Hydrogen Storage Capacity. *J Am Chem Soc* **2022**, *144*, 13729-13739.

[51] Sengupta, D.;Melix, P.;Bose, S.;Duncan, J.;Wang, X. J.;Mian, M. R.;Kirlikovali, K. O.;Joodaki, F.;Islamoglu, T.;Yildirim, T.;Snurr, R. Q.; Farha, O. K. Air-Stable Cu(I) Metal-Organic Framework for Hydrogen Storage. *J Am Chem Soc* **2023**, *145*, 20492-20502.

[52] Suresh, K.;Aulakh, D.;Purewal, J.;Siegel, D. J.;Veenstra, M.; Matzger, A. J. Optimizing Hydrogen Storage in MOFs through Engineering of Crystal Morphology and Control of Crystal Size. *J Am Chem Soc* **2021**, *143*, 10727-10734.

[53] Cabria, I. Grand canonical Monte Carlo simulations of the hydrogen and methane storage capacities of novel but MOFs at room temperature. *Int J Hydrogen Energ* **2024**, *50*, 160-177.

[54] Yu, S.;Li, S. N.;Meng, X. H.;Wan, C. B.; Ju, X. Tuning the hydrogen adsorption properties of Zn-based metal-organic frameworks: Combined DFT and GCMC simulations. *J Solid State Chem* **2018**, *266*, 31-36.

[55] Ahmed, A.;Seth, S.;Purewal, J.;Wong-Foy, A. G.;Veenstra, M.;Matzger, A. J.; Siegel, D. J. Exceptional hydrogen storage achieved by screening nearly half a million metal-organic frameworks. *Nat Commun* **2019**, *10*.

[56] Veccham, S. P.; Head-Gordon, M. Density Functionals for Hydrogen Storage: Defining the H2Bind275 Test Set with Ab Initio Benchmarks and Assessment of 55 Functionals. *J Chem Theory Comput* **2020**, *16*, 4963-4982.

[57] Veccham, S. P.; Head-Gordon, M. Assessment of Performance of Density Functionals for Predicting Potential Energy Curves in Hydrogen Storage Applications. *J Phys Chem A* **2021**, *125*, 4245-4257.

[58] Liu, S. P.;Dupuis, R.;Fan, D.;Benzaria, S.;Bonneau, M.;Bhatt, P.;Eddaoudi, M.; Maurin, G. Machine learning potential for modelling H adsorption/diffusion in MOFs with open metal sites. *Chem Sci* **2024**, *15*, 5294-5302.

[59] Barnett, B. R.;Evans, H. A.;Su, G. M.;Jiang, H. Z. H.;Chakraborty, R.;Banyeretse, D.;Hartman, T. J.;Martinez, M. B.;Trump, B. A.;Tarver, J. D.;Dods, M. N.;Funke, L. M.;Borgel, J.;Reimer, J. A.;Drisdell, W. S.;Hurst, K. E.;Gennett, T.;FitzGerald, S. A.;Brown, C. M.;Head-Gordon, M.; Long, J. R. Observation of an Intermediate to H-2 Binding in a Metal-Organic Framework. *J Am Chem Soc* **2021**, *143*, 14884-14894.

[60] Liu, S. Y.;Zhang, Y.;Zhu, F. Z.;Liu, J. Y.;Wan, X.;Liu, R. A.;Liu, X. F.;Shang, J. X.;Yu, R. H.;Feng, Q.;Wang, Z. L.; Shui, J. L. Mg-MOF-74 Derived Defective Framework for Hydrogen Storage at Above-Ambient Temperature Assisted by Pt Catalyst. *Adv Sci* **2024**, 10.1002/advs.202401868.

[61] Evans, H. A.;Yildirim, T.;Peng, P.;Cheng, Y. Q.;Deng, Z. Y.;Zhang, Q.;Mullangi, D.;Zhao, D.;Canepa, P.;Breunig, H. M.;Cheetham, A. K.; Brown, C. M. Hydrogen Storage with Aluminum Formate, ALF: Experimental, Computational, and Technoeconomic Studies. *J Am Chem Soc* **2023**, *145*, 22150-22157.

[62] Halder, A.;Klein, R. A.;Shulda, S.;McCarver, G. A.;Parilla, P. A.;Furukawa, H.;Brown, C. M.; McGuirk, C. M. Multivariate Flexible Framework with High Usable Hydrogen Capacity in a Reduced Pressure Swing Process. *J Am Chem Soc* **2023**, *145*, 8033-8042.

[63] Senkovska, I.;Bon, V.;Abylgazina, L.;Mendt, M.;Berger, J.;Kieslich, G.;Petkov, P.;Fiorio, J. L.;Joswig, J. O.;Heine, T.;Schaper, L.;Bachetzky, C.;Schmid, R.;Fischer, R. A.;Pöppl, A.;Brunner, E.; Kaskel, S. Understanding MOF Flexibility: An Analysis Focused on Pillared Layer MOFs as a Model System. *Angew Chem Int Edit* **2023**, *62*.

[64] Wieme, J.;Lejaeghere, K.;Kresse, G.; Van Speybroeck, V. Tuning the balance between dispersion and entropy to design temperature-responsive flexible metal-organic frameworks. *Nat Commun* **2018**, *9*.

[65] Coudert, F. X. Molecular Mechanism of Swing Effect in Zeolitic Imidazolate Framework ZIF-8: Continuous Deformation upon Adsorption. *Chemphyschem* **2017**, *18*, 2732-2738.

[66] Krause, S.;Evans, J. D.;Bon, V.;Senkovska, I.;Coudert, F. X.;Többens, D. M.;Wallacher, D.;Grimm, N.; Kaskel, S. The role of temperature and adsorbate on negative gas adsorption transitions of the mesoporous metal-organic framework DUT-49. *Faraday Discuss* **2021**, *225*, 168-183.

[67] Zhang, Y. H.;Wu, S. F.;Wang, L. W.; Zhang, X. F. Chemisorption solid materials for hydrogen storage near ambient temperature: a review. *Front Energy* **2022**, *17*, 72-101.

[68] Berube, V.;Radtke, G.;Dresselhaus, M.; Chen, G. Size effects on the hydrogen storage properties of nanostructured metal hydrides: A review. *Int J Energ Res* **2007**, *31*, 637-663.

[69] Luo, Y.;Wang, Q.;Li, J.;Xu, F.;Sun, L.;Zou, Y.;Chu, H.;Li, B.; Zhang, K. Enhanced hydrogen storage/sensing of metal hydrides by nanomodification. *Mater Today Nano* **2020**, *9*.

[70] Nguyen, H. Q.; Shabani, B. Review of metal hydride hydrogen storage thermal management for use in the fuel cell systems. *Int J Hydrogen Energ* **2021**, *46*, 31699-31726.

[71] Nielsen, T. K.;Besenbacher, F.; Jensen, T. R. Nanoconfined hydrides for energy storage. *Nanoscale* **2011**, *3*, 2086-2098.

[72] Rusman, N. A. A.; Dahari, M. A review on the current progress of metal hydrides material for solid-state hydrogen storage applications. *Int J Hydrogen Energ* **2016**, *41*, 12108-12126.

[73] Sakintuna, B.;Lamari-Darkrim, F.; Hirscher, M. Metal hydride materials for solid hydrogen storage: A review. *Int J Hydrogen Energ* **2007**, *32*, 1121-1140.

[74] Schuth, F.;Bogdanovic, B.; Felderhoff, M. Light metal hydrides and complex hydrides for hydrogen storage. *Chem Commun* **2004**, 10.1039/b406522k, 2249-2258.

[75] Tarasov, B. P.;Fursikov, P. V.;Volodin, A. A.;Bocharnikov, M. S.;Shimkus, Y. Y.;Kashin, A. M.;Yartys, V. A.;Chidziva, S.;Pasupathi, S.; Lototskyy, M. V. Metal hydride hydrogen storage and compression systems for energy storage technologies. *Int J Hydrogen Energ* **2021**, *46*, 13647-13657.

[76] Abdin, Z.;Tang, C. G.;Liu, Y.; Catchpole, K. Large-scale stationary hydrogen storage via liquid organic hydrogen carriers. *Iscience* **2021**, *24*.

[77] Makepeace, J. W.;He, T.;Weidenthaler, C.;Jensen, T. R.;Chang, F.;Vegge, T.;Ngene, P.;Kojima, Y.;de Jongh, P. E.;Chen, P.; David, W. I. F. Reversible ammonia-based and liquid organic hydrogen carriers for high-density hydrogen storage: Recent progress. *Int J Hydrogen Energ* **2019**, *44*, 7746-7767.

[78] Dun, C.;Jeong, S.;Kwon, D. H.;Kang, S.;Stavila, V.;Zhang, Z. L.;Lee, J. W.;Mattox, T. M.;Heo, T. W.;Wood, B. C.; Urban, J. J. Hydrogen Storage Performance of Preferentially Oriented Mg/rGO Hybrids. *Chem Mater* **2022**, *34*, 2963-2971.

[79] Zaluska, A.;Zaluski, L.; Strom-Olsen, J. O. Lithium-beryllium hydrides: the lightest reversible metal hydrides. *J Alloy Compd* **2000**, *307*, 157-166.

[80] Woolf, H.;Brown, I.; Bowden, M. Light metal hydrides - Potential hydrogen storage materials. *Curr Appl Phys* **2008**, *8*, 459-462.

[81] Kawaguchi, M. Kinetic and Fourier Transform Infrared Studies on the Thermal Decomposition of Sodium Hydride. *J Phys Chem C* **2021**, *125*, 11813-11819.

[82] Jain, A.;Miyaoka, H.; Ichikawa, T. Destabilization of lithium hydride by the substitution of group 14 elements: A review. *Int J Hydrogen Energ* **2016**, *41*, 5969-5978.

[83] Dornheim, M.;Doppiu, S.;Barkhordarian, G.;Boesenberg, U.;Klassen, T.;Gutfleisch, O.; Bormann, R. Hydrogen storage in magnesium-based hydrides and hydride composites. *Scripta Mater* **2007**, *56*, 841-846.

[84] Zhu, M.;Wang, H.;Ouyang, L. Z.; Zeng, M. Q. Composite structure and hydrogen storage properties in Mg-base alloys. *Int J Hydrogen Energ* **2006**, *31*, 251-257.

[85] Imamura, H.;Masanari, K.;Kusuhara, M.;Katsumoto, H.;Sumi, T.; Sakata, Y. High hydrogen storage capacity of nanosized magnesium synthesized by high energy ball-milling. *J Alloy Compd* **2005**, *386*, 211-216.

[86] Zaluska, A.;Zaluski, L.; Strom-Olsen, J. O. Structure, catalysis and atomic reactions on the nano-scale: a systematic approach to metal hydrides for hydrogen storage. *Appl Phys a-Mater* **2001**, *72*, 157-165.

[87] Ponthieu, M.;Fernandez, J. F.;Cuevas, F.;Bodega, J.;Ares, J. R.;Adeva, P.; Sanchez, C. Thermodynamics and reaction pathways of hydrogen sorption in Mg-6(Pd,TM) (TM = Ag, Cu and Ni) pseudo-binary compounds. *Int J Hydrogen Energ* **2014**, *39*, 18291-18301.

[88] Hanada, N.;Ichikawa, T.; Fujii, H. Catalytic effect of nanoparticle 3d-transition metals on hydrogen storage properties in magnesium hydride MgH2 prepared by mechanical milling. *J Phys Chem B* **2005**, *109*, 7188-7194.

[89] Darriet, B.;Pezat, M.;Hbika, A.; Hagenmuller, P. Application of Magnesium Rich Rare-Earth Alloys to Hydrogen Storage. *Int J Hydrogen Energ* **1980**, *5*, 173-178.

[90] Bellemare, J.; Huot, J. Hydrogen storage properties of cold rolled magnesium hydrides with oxides catalysts. *J Alloy Compd* **2012**, *512*, 33-38.

[91] Varin, R. A.;Czujko, T.;Chiu, C.; Wronski, Z. Particle size effects on the desorption properties of nanostructured magnesium dihydride (MgH2) synthesized by controlled reactive mechanical milling (CRMM). *J Alloy Compd* **2006**, *424*, 356-364.

[92] Cho, E. S.;Ruminski, A. M.;Liu, Y. S.;Shea, P. T.;Kang, S. Y.;Zaia, E. W.;Park, J. Y.;Chuang, Y. D.;Yuk, J. M.;Zhou, X. W.;Heo, T. W.;Guo, J. H.;Wood, B. C.; Urban, J. J. Hierarchically Controlled Inside-Out Doping of Mg Nanocomposites for Moderate Temperature Hydrogen Storage. *Adv Funct Mater* **2017**, *27*.

[93] Ruminski, A. M.;Bardhan, R.;Brand, A.;Aloni, S.; Urban, J. J. Synergistic enhancement of hydrogen storage and air stability via Mg nanocrystal-polymer interfacial interactions. *Energ Environ Sci* **2013**, *6*, 3267-3271.

[94] Jeon, K. J.;Moon, H. R.;Ruminski, A. M.;Jiang, B.;Kisielowski, C.;Bardhan, R.; Urban, J. J. Air-stable magnesium nanocomposites provide rapid and high-capacity hydrogen storage without using heavy-metal catalysts. *Nat Mater* **2011**, *10*, 286-290.

[95] Jeong, S.;Heo, T. W.;Oktawiec, J.;Shi, R. P.;Kang, S.;White, J. L.;Schneemann, A.;Zaia, E. W.;Wan, L. W. F.;Ray, K. G.;Liu, Y. S.;Stavila, V.;Guo, J. H.;Long, J. R.;Wood, B. C.; Urban, J. J. A Mechanistic Analysis of Phase Evolution and Hydrogen Storage Behavior in Nanocrystalline Mg(BH4)(2) within Reduced Graphene Oxide. *Acs Nano* **2020**, *14*, 1745-1756.

[96] Wan, L. W.;Li, Y. S.;Cho, E. S.;Forster, J.;Jeong, S.;Wang, H. T.;Urban, J.;Guo, J. H.; Prendergast, D. Atomically thin interfacial suboxide key to hydrogen storage performance

enhancements of magnesium nanoparticles encapsulated in reduced graphene oxide. *Abstr Pap Am Chem S* **2018**, *255*.

[97] Wan, L. W. F.;Cho, E. S.;Marangoni, T.;Shea, P.;Kang, S.;Rogers, C.;Zaia, E.;Cloke, R. R.;Wood, B. C.;Fischer, F. R.;Urban, J. J.; Prendergast, D. Edge-Functionalized Graphene Nanoribbon Encapsulation To Enhance Stability and Control Kinetics of Hydrogen Storage Materials. *Chem Mater* **2019**, *31*, 2960-2970.

[98] Zhang, Z. L.;Su, J.;Matias, A. S.;Gordon, M.;Liu, Y. S.;Guo, J. H.;Song, C. Y.;Dun, C. C.;Prendergast, D.;Somorjai, G. A.; Urban, J. J. Enhanced and stabilized hydrogen production from methanol by ultrasmall Ni nanoclusters immobilized on defect-rich h-BN nanosheets. *P Natl Acad Sci USA* **2020**, *117*, 29442-29452.

[99] Ruminski, A. M.;Bardhan, R.;Brand, A.;Aloni, S.; Urban, J. J. Synergistic enhancement of hydrogen storage and air stability

Mg nanocrystal-polymer interfacial interactions. *Energ Environ Sci* **2013**, *6*, 3267-3271.

[100] Cho, E. S.;Ruminski, A. M.;Aloni, S.;Liu, Y. S.;Guo, J. H.; Urban, J. J. Graphene oxide/metal nanocrystal multilaminates as the atomic limit for safe and selective hydrogen storage (vol 7, 10804, 2016). *Nat Commun* **2016**, *7*.

[101] Wan, L. W. F.;Liu, Y. S.;Cho, E. S.;Forster, J. D.;Jeong, S.;Wang, H. T.;Urban, J. J.;Guo, J. H.; Prendergast, D. Atomically Thin Interfacial Suboxide Key to Hydrogen Storage Performance Enhancements of Magnesium Nanoparticles Encapsulated in Reduced Graphene Oxide. *Nano Lett* **2017**, *17*, 5540-5545.

[102] Seayad, A. M.; Antonelli, D. M. Recent advances in hydrogen storage in metal-containing inorganic nanostructures and related materials. *Adv Mater* **2004**, *16*, 765-777.

[103] Zhao, L.;Xu, F.;Zhang, C. C.;Wang, Z. Y.;Ju, H. Y.;Gao, X.;Zhang, X. X.;Sun, L. X.; Liu, Z. W. Enhanced hydrogen storage of alanates: Recent progress and future perspectives. *Prog Nat Sci-Mater* **2021**, *31*, 165-179.

[104] Kang, S.;Heo, T. W.;Allendorf, M. D.; Wood, B. C. Morphology-Dependent Stability of Complex Metal Hydrides and Their Intermediates Using First-Principles Calculations. *Chemphyschem* **2019**, *20*, 1340-1347.

[105] Dun, C.;Li, S. C.;Chen, L. F.;Horton, R. D.;Allendorf, M. D.;Wood, B. C.;Stavila, V.; Urban, J. J. A Nanoscale Ternary Amide-rGO Composite with Boosted Kinetics for Reversible H2 Storage. *Adv Mater Interfaces* **2023**, *10*.

[106] Stavila, V.;Li, S. C.;Dun, C.;Marple, M. A. T.;Mason, H. E.;Snider, J. L.;Reynolds, J. E.;El Gabaly, F.;Sugar, J. D.;Spataru, C. D.;Zhou, X. W.;Dizdar, B.;Majzoub, E. H.;Chatterjee, R.;Yano, J.;Schlomberg, H.;Lotsch, B. V.;Urban, J. J.;Wood, B. C.; Allendorf, M. D. Defying Thermodynamics: Stabilization of Alane Within Covalent Triazine Frameworks for Reversible Hydrogen Storage. *Angew Chem Int Edit* **2021**, *60*, 25815-25824.

[107] Gunda, H.;Ray, K. G.;Klebanoff, L. E.;Dun, C.;Marple, M. A. T.;Li, S. C.;Sharma, P.;Friddle, R. W.;Sugar, J. D.;Snider, J. L.;Horton, R. D.;Davis, B. C.;Chames, J. M.;Liu, Y. S.;Guo, J. H.;Mason, H. E.;Urban, J. J.;Wood, B. C.;Allendorf, M. D.;Jasuja, K.; Stavila, V. Hydrogen Storage in Partially Exfoliated Magnesium Diboride Multilayers. *Small* **2023**, *19*.

[108] Zhang, J. Y.;Wang, W. D.;Chen, X. W.;Jin, J. L.;Yan, X. J.; Huang, J. M. Single-Atom Ni Supported on TiO for Catalyzing Hydrogen Storage in MgH. *J Am Chem Soc* **2024**, *146*, 10432-10442.

[109] Balcerzak, M.;Ponsoni, J. B.;Petersen, H.;Menéndez, C.;Ternieden, J.;Zhang, L. D.;Winkelmann, F.;Aguey-Zinsou, K. F.;Hirscher, M.; Felderhoff, M. Hydrogen-Stabilized ScYNdGd Medium-Entropy Alloy for Hydrogen Storage. *J Am Chem Soc* **2024**, *146*, 5283-5294.

[110] Kostiuchenko, T.;Körmann, F.;Neugebauer, J.; Shapeev, A. Impact of lattice relaxations on phase transitions in a high-entropy alloy studied by machine-learning potentials. *Npj Comput Mater* **2019**, *5*.

[111] Witman, M.;Ek, G.;Ling, S. L.;Chames, J.;Agarwal, S.;Wong, J.;Allendorf, M. D.;Sahlberg, M.; Stavila, V. Data-Driven Discovery and Synthesis of High Entropy Alloy Hydrides with Targeted Thermodynamic Stability. *Chem Mater* **2021**, *33*, 4067-4076.

[112] Moosavi, S. M.;Jablonka, K. M.; Smit, B. The Role of Machine Learning in the Understanding and Design of Materials. *J Am Chem Soc* **2020**, *142*, 20273-20287.

[113] Jablonka, K. M.;Ongari, D.;Moosavi, S. M.; Smit, B. Using collective knowledge to assign oxidation states of metal cations in metal-organic frameworks. *Nat Chem* **2021**, *13*, 771-+.

[114] Moosavi, S. M.;Novotny, B. A.;Ongari, D.;Moubarak, E.;Asgari, M.;Kadioglu, Ö.;Charalambous, C.;Ortega-Guerrero, A.;Farmahini, A. H.;Sarkisov, L.;Garcia, S.;Noé, F.; Smit, B. A data-science approach to predict the heat capacity of nanoporous materials. *Nat Mater* **2022**, *21*, 1419-+.

[115] Liu, S. Y.;Liu, J. Y.;Liu, X. F.;Shang, J. X.;Xu, L.;Yu, R. H.; Shui, J. L. Hydrogen storage in incompletely etched multilayer TiCT at room temperature. *Nat Nanotechnol* **2021**, *16*, 331-336.

[116] Andersson, J.; Grönkvist, S. Large-scale storage of hydrogen. *Int J Hydrogen Energ* **2019**, *44*, 11901-11919.

[117] Sathe, R. Y.;Kumar, T. J. D.; Ahuja, R. Furtherance of the material-based hydrogen storage based on theory and experiments. *Int J Hydrogen Energ* **2023**, *48*, 12767-12795.

[118] Bevan, A. I.;Züttel, A.;Book, D.; Harris, I. R. Performance of a metal hydride store on the "Ross Barlow" hydrogen powered canal boat. *Faraday Discuss* **2011**, *151*, 353-367.

[119] Broom, D. P.;Webb, C. J.;Fanourgakis, G. S.;Froudakis, G. E.;Trikalitis, P. N.; Hirscher, M. Concepts for improving hydrogen storage in nanoporous materials. *Int J Hydrogen Energ* **2019**, *44*, 7768-7779.

[120] Mostafa, M. H.;Aleem, S. H. E. A.;Ali, S. G.;Ali, Z. M.; Abdelaziz, A. Y. Techno-economic assessment of energy storage systems using annualized life cycle cost of storage (LCCOS) and levelized cost of energy (LCOE) metrics. *J Energy Storage* **2020**, *29*.

[121] Hunter, C. A.;Penev, M. M.;Reznicek, E. P.;Eichman, J.;Rustagi, N.; Baldwin, S. F. Techno-economic analysis of long-duration energy storage and flexible power generation technologies to support high-variable renewable energy grids. *Joule* **2021**, *5*, 2077-2101.

[122] Peng, P.;Anastasopoulou, A.;Brooks, K.;Furukawa, H.;Bowden, M. E.;Long, J. R.;Autrey, T.; Breunig, H. Cost and potential of metal-organic frameworks for hydrogen back-up power supply. *Nat Energy* **2022**, *7*, 448-458.

[123] Ahluwalia, R. K.;Peng, J. K.; Hua, T. Q. Sorbent material property requirements for on-board hydrogen storage for automotive fuel cell systems. *Int J Hydrogen Energ* **2015**, *40*, 6373-6390.

[124] Nguyen, D. H.;Kim, J. H.;Vo, T. T. N.;Kim, N.; Ahn, H. S. Design of portable hydrogen tank using adsorption material as storage media: An alternative to Type IV compressed tank. *Appl Energ* **2022**, *310*.

[125] Grady, C.;McWhorter, S.;Sulic, M.;Sprik, S. J.;Thornton, M. J.;Brooks, K. P.; Tamburello, D. A. Design tool for estimating adsorbent hydrogen storage system characteristics for light-duty fuel cell vehicles. *Int J Hydrogen Energ* **2022**, *47*, 29847-29857.

[126] Brooks, K. P.;Sprik, S. J.;Tamburello, D. A.; Thornton, M. J. Design tool for estimating metal hydride storage system characteristics for light-duty hydrogen fuel cell vehicles. *Int J Hydrogen Energ* **2020**, *45*, 24917-24927.

[127] Anastasopoulou, A.;Furukawa, H.;Barnett, B. R.;Jiang, H. Z. H.;Long, J. R.; Breunig, H. M. Technoeconomic analysis of metal-organic frameworks for bulk hydrogen transportation. *Energ Environ Sci* **2021**, *14*, 1083-1094.

[128] Pasini, J. M.;Corgnale, C.;van Hassel, B. A.;Motyka, T.;Kumar, S.; Simmons, K. L. Metal hydride material requirements for automotive hydrogen storage systems. *Int J Hydrogen Energ* **2013**, *38*, 9755-9765.

[129] Klopcic, N.;Grimmer, I.;Winkler, F.;Sartory, M.; Trattner, A. A review on metal hydride materials for hydrogen storage. *J Energy Storage* **2023**, *72*.

[130] van Hassel, B. A.;Mosher, D.;Pasini, J. M.;Gorbounov, M.;Holowczak, J.;Tang, X.;Brown, R.;Laube, B.; Pryor, L. Engineering improvement of NaAlHsystem. *Int J Hydrogen Energ* **2012**, *37*, 2756-2766.

[131] Amica, G.;Larochette, P. A.; Gennari, F. C. Light metal hydride-based hydrogen storage system: Economic assessment in Argentina. *Int J Hydrogen Energ* **2020**, *45*, 18789-18801.

[132] Zhang, B.; Wu, Y. Recent advances in improving performances of the lightweight complex hydrides Li-Mg-N-H system. *Prog Nat Sci-Mater* **2017**, *27*, 21-33.

[133] Xu, Z.;Zhao, N.;Hillmansen, S.;Roberts, C.; Yan, Y. Techno-Economic Analysis of Hydrogen Storage Technologies for Railway Engineering: A Review. *Energies* **2022**, *15*.

[134] Lapeña-Rey, N.;Blanco, J. A.;Ferreyra, E.;Lemus, J. L.;Pereira, S.; Serrot, E. A fuel cell powered unmanned aerial vehicle for low altitude surveillance missions. *Int J Hydrogen Energ* **2017**, *42*, 6926-6940.

[135] Psoma, A.; Sattler, G. Fuel cell systems for submarines: from the first idea to serial production. *J Power Sources* **2002**, *106*, 381-383.

[136] Fiori, C.;Dell'Era, A.;Zuccari, F.;Santiangeli, A.;D'Orazio, A.; Orecchini, F. Hydrides for submarine applications: Overview and identification of optimal alloys for air independent propulsion maximization. *Int J Hydrogen Energ* **2015**, *40*, 11879-11889.

[137] Danebergs, J.; Deledda, S. Can hydrogen storage in metal hydrides be economically competitive with compressed and liquid hydrogen storage? A techno-economical perspective for the maritime sector. *Int J Hydrogen Energ* **2024**, *50*, 1040-1054.

[138] Drawer, C.;Lange, J.; Kaltschmitt, M. Metal hydrides for hydrogen storage - Identification and evaluation of stationary and transportation applications. *J Energy Storage* **2024**, *77*.

[139] DeSantis, D.;Mason, J. A.;James, B. D.;Houchins, C.;Long, J. R.; Veenstra, M. Techno-economic Analysis of Metal-Organic Frameworks for Hydrogen and Natural Gas Storage. *Energ Fuel* **2017**, *31*, 2024-2032.

[140] Luo, H. X.;Cheng, F. W.;Huelsenbeck, L.; Smith, N. Comparison between conventional solvothermal and aqueous solution-based production of UiO-66-NH: Life cycle assessment, techno-economic assessment, and implications for CO capture and storage. *J Environ Chem Eng* **2021**, *9*.

[141] Modi, P.; Aguey-Zinsou, K. F. Room Temperature Metal Hydrides for Stationary and Heat Storage Applications: A Review. *Front Energy Res* **2021**, *9*.

[142] Ahmadi, N.;Dadvand, A.;Rezazadeh, S.; Mirzaee, I. Analysis of the operating pressure and GDL geometrical configuration effect on PEM fuel cell performance. *J Braz Soc Mech Sci* **2016**, *38*, 2311-2325.

[143] Hancke, R.;Holm, T.; Ulleberg, O. The case for high-pressure PEM water electrolysis. *Energ Convers Manage* **2022**, *261*.

[144] von Colbe, J. B.;Ares, J. R.;Barale, J.;Baricco, M.;Buckley, C.;Capurso, G.;Gallandat, N.;Grant, D. M.;Guzik, M. N.;Jacob, I.;Jensen, E. H.;Jensen, T.;Jepsen, J.;Klassen, T.;Lototskyy, M. V.;Manickam, K.;Montone, A.;Puszkiel, J.;Sartori, S.;Sheppard, D. A.;Stuart, A.;Walker, G.;Webb, C. J.;Yang, H.;Yartys, V.;Züttel, A.; Dornheim, M. Application of hydrides in hydrogen storage and compression: Achievements, outlook and perspectives. *Int J Hydrogen Energ* **2019**, *44*, 7780-7808.

[145] Wilmer, C. E.; Snurr, R. Q. Large-Scale Generation and Screening of Hypothetical Metal-Organic Frameworks for Applications in Gas Storage and Separations. *Top Curr Chem* **2014**, *345*, 257-289.

[146] Kim, S. Y.;Kim, S. I.; Bae, Y. S. Machine-Learning-Based Prediction of Methane Adsorption Isotherms at Varied Temperatures for Experimental Adsorbents. *J Phys Chem C* **2020**, *124*, 19538-19547.

[147] Chong, S.;Lee, S.;Kim, B.; Kim, J. Applications of machine learning in metal-organic frameworks. *Coordin Chem Rev* **2020**, *423*.

[148] Demir, H.;Daglar, H.;Gulbalkan, H. C.;Aksu, G. O.; Keskin, S. Recent advances in computational modeling of MOFs: From molecular simulations to machine learning. *Coordin Chem Rev* **2023**, *484*.

[149] Lu, X. Y.;Xie, Z. Z.;Wu, X. J.;Li, M. M.; Cai, W. Q. Hydrogen storage metal-organic framework classification models based on crystal graph convolutional neural networks. *Chem Eng Sci* **2022**, *259*.

[150] Rahnama, A.;Zepon, G.; Sridhar, S. Machine learning based prediction of metal hydrides for hydrogen storage, part I: Prediction of hydrogen weight percent. *Int J Hydrogen Energ* **2019**, *44*, 7337-7344.

[151] Witman, M.;Ling, S. L.;Grant, D. M.;Walker, G. S.;Agarwal, S.;Stavila, V.; Allendorf, M. D. Extracting an Empirical Intermetallic Hydride Design Principle from Limited Data via Interpretable Machine Learning. *J Phys Chem Lett* **2020**, *11*, 40-47.

[152] Broom, D. P.; Hirscher, M. Irreproducibility in hydrogen storage material research. *Energ Environ Sci* **2016**, *9*, 3368-3380.

[153] Barale, J.;Dematteis, E. M.;Capurso, G.;Neuman, B.;Deledda, S.;Rizzi, P.;Cuevas, F.; Baricco, M. TiFe0.85Mn0.05 alloy produced at industrial level for a hydrogen storage plant. *Int J Hydrogen Energ* **2022**, *47*, 29866-29880.

[154] Chung, Y. G.;Haldoupis, E.;Bucior, B. J.;Haranczyk, M.;Lee, S.;Zhang, H. D.;Vogiatzis, K. D.;Milisavljevic, M.;Ling, S. L.;Camp, J. S.;Slater, B.;Siepmann, J. I.;Sholl, D. S.; Snurr, R. Q. Advances, Updates, and Analytics for the Computation-Ready, Experimental Metal-Organic Framework Database: CoRE MOF 2019. *J Chem Eng Data* **2019**, *64*, 5985-5998.

[155] Li, Q.;Lu, Y. F.;Luo, Q.;Yang, X. H.;Yang, Y.;Tan, J.;Dong, Z. H.;Dang, J.;Li, J. B.;Chen, Y.;Jiang, B.;Sun, S. H.; Pan, F. S. Thermodynamics and kinetics of hydriding and dehydriding reactions in Mg-based hydrogen storage materials. *J Magnes Alloy* **2021**, *9*, 1922-1941.